2010-11-03

MIMO Channel Spatial Covariance Estimation: Analysis Using a Closed-Form Model

Yanling Yang
Brigham Young University - Provo

MIMO Channel Spatial Covariance Estimation:

Analysis Using a Closed-Form Model

Yanling Yang

A thesis submitted to the faculty of
Brigham Young University
in partial fulfillment of the requirements for the degree of

Master of Science

Michael A. Jensen, Chair
Brian D. Jeffs
Karl F. Warnick

Department of Electrical and Computer Engineering

Brigham Young University

December 2010

ABSTRACT

MIMO Channel Spatial Covariance Estimation:

Analysis Using a Closed-Form Model

Yanling Yang

Department of Electrical and Computer Engineering

Master of Science

Multiple-input Multiple-output (MIMO) wireless communication systems allow increased spectral efficiency and therefore promise significant improvement in performance. However, because of the rapid variation in channel state information (CSI) in networks with mobile nodes or scatterers, it is difficult both to maintain high communication performance and to create channel models that effectively represent the time-varying behavior of the channels. The spatial covariance of the MIMO channel describes the average power gain on each transmit-receive antenna pair as well as the correlation between the complex link gains and thus provides critical information for understanding the performance of the system and for creating models to accurately describe the interaction of the electromagnetic fields with the antennas. Furthermore, in many cases the MIMO signaling scheme uses knowledge of this spatial covariance. This thesis proposes a closed-form analytical model that allows estimation of the full MIMO channel covariance based on knowledge of the power angular spectrum (PAS) of the channel and the antenna radiation patterns. Comparison of covariance matrices computed using this model with those estimated from observed channel samples reveals the appropriate window over which the covariance should be estimated for non-WSS time-varying channels. Two approaches are developed to compare the covariance matrices in order to determine the appropriate window, both based on a metric, correlation matrix distance (CMD). Simulations based on both a two-ring propagation model and ray-tracing data in a three dimensional urban environment are included. The results reveal that with the optimal window size, the CMD of the estimated covariance is close to that of the analytical covariance. An average window size normalized by the scatterer circle radius is determined for practical estimation of covariance based on knowledge of the average distance to the scatterers. The impact of the number of scatterers on the optimal window size is analyzed as well. The results based on ray-tracing data show that the CMD of the estimated covariance using a $16 - 17\lambda$ window match the CMD of the analytical covariance.

Keywords: MIMO system, channel spatial covariance, model

ACKNOWLEDGMENTS

I would like to thank my advisor, Dr. Michael A. Jensen, for his time and advice in researching and writing about this topic, to whom I owe a great amount of gratitude for his patience and guidance during my education. I am also very grateful to all of the faculty and staff who have helped me from my admission till my graduation. Last but not the least, I would like to thank my husband, Huili Yu, who has always supported me both in my study and in my life.

Table of Contents

List of Tables

List of Figures

Chapter 1

Introduction

Multipath fading represents a significant challenge in the implementation of reliable wireless communication systems. For many years, the development community has recognized that using multiple antennas at the transmitter or the receiver can help overcome the detrimental effects of fading using a technique known as antenna diversity. More recently, research has shown that using multiple antennas at both ends of the link, a configuration referred to as multiple-input multiple-output (MIMO), can dramatically enhance the achievable channel capacity [1, 2]. This is achieved either by exploiting combined transmit and receive diversity or by sending multiple simultaneous data streams across the channel.

While the potential for increased capacity in MIMO wireless systems has been demonstrated in many recent publications [3, 4], research has also shown that practical issues, such as the time-varying behavior of the channel and how well it can be tracked at both the receiver and the transmitter, can dramatically impact the potential throughput gains realized using MIMO techniques [5]. Therefore, successful implementation of a MIMO system with high performance requires careful consideration of several key elements.

Among these key elements, the signaling strategy used and proper understanding of the propagation channel are particularly important since they are closely related to the realistic system assumptions. In a MIMO system operating in a time-varying channel, it is difficult to track the changing channel at the receiver and even more difficult to provide updated information to the transmitter. It is also challenging to construct an accurate model representing dynamic propagation conditions in such a channel. Motivated by these observations, past research has demonstrated that by signaling based on the channel spatial covariance matrix rather than the channel state information (CSI), improved communication stability is enabled with reduced channel estimation and feedback requirements [5, 6, 7].

Furthermore, the understanding of how the channel covariance varies in time is useful when trying to understand the dynamic nature of MIMO channels and capture this behavior in a practical model [8, 9].

Despite the importance of the channel spatial covariance matrix in MIMO systems, the calculation of this quantity and its general properties are not well understood for many practical environments [10]. Typically, the covariance matrix is computed using a time average or sample mean of the channel realizations [11, 12], without a determination or a qualification of the window size used. Since channel covariance information depends on the spatial structure of the multipaths, which naturally evolves with communication node motion, then clearly the underlying channel cannot be considered a statistically wide-sense stationary (WSS) process [13]. Therefore, when estimating the covariance from data measured over a range of positions, the spatial window over which the expectation should be performed is poorly defined. Further analysis of this implication for MIMO system design and implementation is therefore required.

1.1 Thesis Contributions

Motivated by the limitations of prior work, this thesis estimates the MIMO channel spatial covariance using a closed-form formulation that allows estimation of the full MIMO covariance based on knowledge of the power angular spectrum (PAS) of the channel and the antenna radiation patterns. This allows us to understand the behavior of the channel covariance as a function of communication node position. The thesis also explores the appropriate size of the spatial window over which the covariance should be estimated for non-WSS time-varying channels using simulations based on simple and realistic propagation models. The main contributions of this thesis are:

1. The derivation of a closed-form analytical covariance model allowing estimation of the full MIMO channel spatial covariance as opposed to the more traditional one-sided or separable covariance.

2. An analysis of the behavior of the spatial channel covariance for time-varying MIMO channels.

3. The exploration of the spatial dependence of the channel spatial covariance, resulting in a necessary understanding for meaningfully generating MIMO channel models.

4. The development and implementation of two algorithms to match the covariance computed from analytical model with that estimated using expectation over a spatial window, with simulation results providing a useful definition of the size of the spatial window.

1.2 Thesis Organization

The remainder of this thesis is organized as follows. Chapter 2 provides background information essential to the understanding of the topics contained in this thesis. This includes discussions on the MIMO system models as well as the channel spatial covariance and its importance in MIMO system design. The Chapter also contains a section that discusses the channel wide-sense stationarity violation.

Chapter 3 derives a closed-form analytical covariance model that allows the estimation of the full MIMO channel spatial covariance based on knowledge of the channel multipath structure. A metric for quantifying non-stationarity, correlation matrix distance (CMD), is introduced in Chapter 3 as well. The Chapter concludes with an example simulation using the analytical model and the CMD to explore the evolution properties of MIMO channels based on a two-ring propagation model.

In Chapter 4, two methods for determining an appropriate window size for covariance estimation are discussed, both based on the CMD. The first method quantifies the average time variation of the covariance and finds the window such that the average derivative of the CMD obtained using the covariance estimated from a sample mean over a window matches that obtained from the analytical covariance. The second method uses a similar approach, finding the window size that minimizes the mean squared error between the CMD curves.

Simulations based on a two-ring propagation model and on ray-tracing data in an urban environment are demonstrated in Chapter 5. Simulation results of CMD agreement are analyzed and conclusions about the impact of environment on the optimal window size are drawn. Chapter 6 summarizes the content of the previous chapters, explains the contributions of this work, and provides recommendations for future work.

Chapter 2

Background

In recent years, multiple-input multiple-output (MIMO) wireless systems that use multiple transmit and receive antennas for communicating over multipath channels have demonstrated significant performance benefits[2, 5]. It is widely understood that the spatial properties of the multipath channels can be used to enhance capacity. However, the capacity highly depends on how well the channel state information (CSI) is known at the transmitter and/or receiver. When the channel is time-varying, outdated CSI results in significant capacity degradation. Research has shown that the capacity obtained using the channel distribution information (CDI) in the form of channel spatial covariance matrices, which characterizes the average power gain on each transmit-receive antenna pair as well as the correlation between complex path gains, has much lower sensitivity to CSI quality due to the fact that the CDI remains more constant with time. Thus, many MIMO systems use knowledge of the spatial covariance to design the signaling schemes. Moreover, the channel spatial covariance provides critical information for studying the performance of the MIMO system and for defining models to accurately describe the interaction of the electromagnetic fields with the antennas. Therefore, the study of the behavior of the channel covariance and its modeling has become an important pursuit in MIMO system research.

This chapter briefly introduces basic MIMO systems and several associated issues, such as channel covariance, the importance of the channel covariance in time-varying MIMO channels, conventional channel covariance models and channel wide-sense stationarity violation.

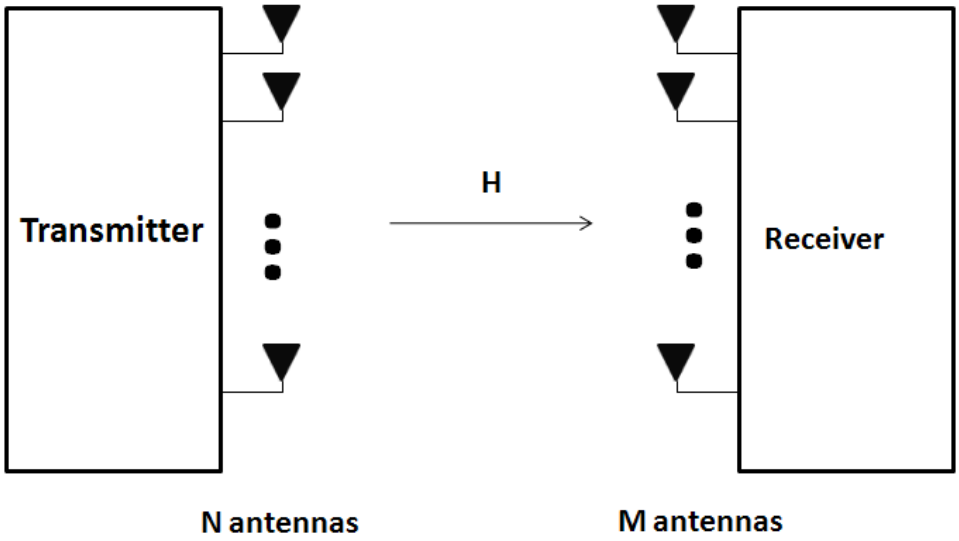

Figure 2.1: A single-user MIMO point to point channel system model.

2.1 MIMO System Model

A single-user MIMO system, shown in Figure 2.1, typically consists of a transmitter with N antennas and a receiver with M antennas [7]. The channel can be represented by the $M \times N$ matrix $\mathbf{H}$. The $M \times 1$ received signal vector $\mathbf{r}$ can be written as

$$\mathbf{r} = \mathbf{H}\mathbf{s} + \mathbf{w}, \tag{2.1}$$

where $\mathbf{s}$ is the $N \times 1$ transmitted vector and $\mathbf{w}$ is the $M \times 1$ vector of additive white Gaussian noise with zero-mean and unit-variance.

Multiuser MIMO systems are often described by two models: the MIMO broadcast channel (BC) and the MIMO multiple-access channel (MAC). The MIMO BC system represents a downlink communication where a single transmitter communicates with multiple receivers. The MIMO MAC represents a MIMO uplink communication where multiple transmitters communicate with a single receiver.

This work focuses on the MIMO BC, which consists of a single transmitting node with N_t antennas and N_u receiving nodes each with N_r antennas [14], as depicted in Figure 2.2. Let $\mathbf{H}_j$ be the $N_r \times N_t$ channel matrix from the transmitter to the jth user. The $N_r \times 1$

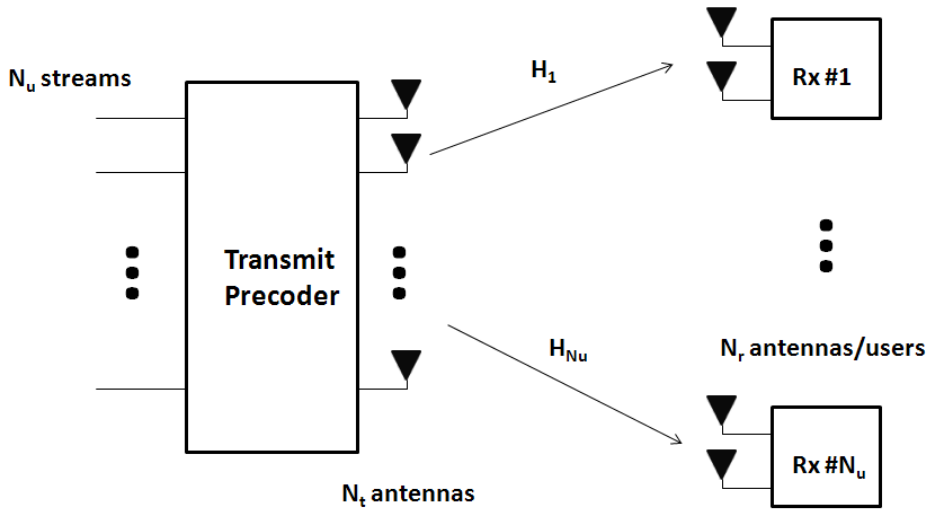

Figure 2.2: A multi-user MIMO broadcast channel system model.

received signal vector for the jth user is given by

$$y_j = \mathbf{H}_j \mathbf{x}_j + \sum_{i=1, i \neq j}^{N_u} \mathbf{H}_j \mathbf{x}_i + \mathbf{n}_j, \tag{2.2}$$

where x_j represents the $N_t \times 1$ precoded vector destined for the jth user and $\mathbf{n}_j$ is the noise vector of zero-mean unit-variance additive white Gaussian random variables.

2.2 Channel Covariance

The channel matrix $\mathbf{H}$ is highly sensitive to small changes in the location of either the transmitter or receiver or to small perturbations in the channel. In contrast, the channel spatial covariance remains relatively constant over reasonable distances (if the channel can be represented by a quasi-stationary process). Thus, recent work has suggested a beamforming strategy based on channel covariance [7, 15]. In this work, the channel covariance is defined as

$$\mathbf{R} = E\{\mathbf{h}\mathbf{h}^\dagger\}, \tag{2.3}$$

where $\mathbf{h} = vec\{\mathbf{H}\}$ and $vec\{\cdot\}$ indicates a column-wise stacking of a matrix into a vector, $E\{\cdot\}$ denotes the expectation, and $\{\cdot\}^\dagger$ is a conjugate transpose. In the MIMO BC described

above, the channel covariance $\mathbf{R}_j$ of each channel is given by

$$\mathbf{R}_j = E\{\mathbf{h}_j \mathbf{h}_j^{\dagger}\}, \tag{2.4}$$

where $\mathbf{h}_j = vec\{\mathbf{H}_j\}$.

2.3 Importance of Channel Spatial Covariance

In a MIMO system, the channel spatial covariance characterizes the average power gain in each channel and the correlation between complex link gains. Thus, it provides essential information for understanding the performance of the MIMO system and for constructing models to accurately describe the properties of the channels. Moreover, in many cases the MIMO signaling scheme requires knowledge of the channel spatial covariance. It has long been found that unlike single antenna systems in which utilizing channel state information at the transmitter (CSIT) does not highly increase the channel capacity, in multiple antenna systems capacity improvement through CSIT can be significant [7]. Assuming that the receiver and transmitter both have accurate CSI and that the channel is time invariant, in a single-user or a multi-user MIMO system, impressive performance potential can be achieved by exploiting optimal MIMO precoding strategies based on instantaneous CSI feedback [11]. However, in most of the wireless communication scenarios with mobile communication nodes, especially in wireless MIMO communication systems, the assumption of time invariance is unrealistic. In fact, in many practical scenarios, the channel varies so rapidly that it becomes difficult and costly to feedback enough information from the receivers to the transmitter to ensure that the transmitter maintains accurate CSI.

Fortunately, the relative geometry of the propagation paths changes more slowly [12], a feature that is characterized by the channel distribution information (CDI), often referred to as partial CSI. Table 2.1 shows the differences between CSI and CDI. When the channel is assumed to be a Gaussian process, the statistics of the channel are reduced to the mean and covariance[16]. Therefore, it is often more realistic to assume that the receiver can perfectly estimate the current CSI, while the transmitter has only the statistics of the channel, such as the channel covariance information.

Unlike CSI which varies quickly in time, channel spatial covariance changes more slowly and can be fed back to the transmitter at a much lower rate. As a result, precoding based on this CDI offers improved temporal stability[11]. Recent analysis of the capacity resulting from channel covariance feedback indicates substantial gain over that achievable without precoding[12]. Moreover, these results imply that for point-to-point links, the beamforming strategy performance is close to that of the optimal strategy when there is a dominant path present.

Extension of transmit precoding based on CDI to the time-variant, multi-user MIMO BC has recently been reported[11]. This work demonstrated that while CDI precoding suffers performance loss relative to that achievable using CSI precoding, under time varying conditions and for reasonable feedback intervals, it offers improved performance on average. The paper further developed a method for parameterizing the required CDI using two commonly accepted channel models, namely the Kronecker and Weichselberger models. The simulations in the paper showed that this parameterization algorithm reduced the feedback on par with CSI-based schemes with minor loss in throughput performance while significantly decreasing the frequency of the feedback.

Based on these discussions, we can conclude that channel covariance estimation from channel observations has become a valuable aspect of MIMO system research and implementation.

2.4 Conventional Correlation-based Channel Models

With the increased use of wireless MIMO technology, the need for accurately describing the spatial domain of the channels has become ever more apparent. There exist many channel models aimed at capturing these spatial properties, such as propagation-based de-

Table 2.1: Comparison between CSI and CDI (Spatial covariance).

CSI	CDI (Spatial covariance)
• Depends on multipath superposition	• Depends on multipath spatial structure
• Varies rapidly with node position	• Varies slowly with node position
• Significant feedback frequency for Tx CSI	• Reduced feedback frequency for Tx CDI

terministic models, geometry-based stochastic models and some analytical models. Among the analytical models, one group consists of the correlation-based channel models that first try to represent the spatial correlation between MIMO channels. The most popular such model represents the correlation matrix through a Kronecker product[17].

These analytical models of the MIMO channels focus on modeling the underlying spatial correlation structure of the MIMO channels [18]. They are convenient matrix representations of the MIMO channels which can be used in the analytical design of precoding strategies. However, physical models or data are still required to be used as input when using an analytical model in simulations.

2.4.1 Full Correlation Model

Before we introduce the most popular correlation-based models, we focus on the full correlation model. It uses the full spatial correlation matrix defined by Equation (2.3) to model the behavior in the channels. In this model, channel realizations are generated using

$$\mathbf{H}_{corr} = mat\{\sqrt{\mathbf{R}}vec\{\mathbf{H}_w\}\}, \tag{2.5}$$

where *mat* represents the inverse of the *vec* operation and $\mathbf{H}_w$ is an $N_r \times N_t$ matrix with zero-mean, unit variance, i.i.d. complex Gaussian entries.

The beamforming algorithm based on CDI requires the input parameters $\mathbf{S}_r$ and $\mathbf{S}_t$, which represent nonlinear permutations of the large spatial correlation matrix $\mathbf{R}$ [11]. Typically, $\mathbf{S}_r$ and $\mathbf{S}_t$ are defined by

$$\mathbf{S}_r = E\{\mathbf{H}^* \otimes \mathbf{H}\}, \tag{2.6}$$

$$\mathbf{S}_t = E\{\mathbf{H}^T \otimes \mathbf{H}^\dagger\}, \tag{2.7}$$

where the user subscript has been dropped for notational simplicity and $\{\cdot\}^T$ and $\{\cdot\}^*$ indicate transpose and conjugate respectively. Given the full correlation model, the covariance parameters $\mathbf{S}_r$ and $\mathbf{S}_t$ can be estimated directly from $\mathbf{H}_{corr}$.

Even though the full correlation model has high accuracy, it is usually too complex to be used in practice. If this matrix must be fed back to the transmitter, the complexity is $(N_r N_t)^2$ complex numbers. For this reason, researchers have explored other correlation-based models with a reasonable performance-complexity compromise while being useful in practical applications.

2.4.2 Kronecker Model

One of the most common reduced-complexity representations of the correlation matrix is based on the Kronecker product[19] of component matrices that represent the correlation at the transmitter and receiver. The channel realizations can be generated by

$$\mathbf{H}_{kron} = \sqrt{\mathbf{R}_r}\mathbf{H}_w\sqrt{\mathbf{R}_t}, \tag{2.8}$$

where the one-sided correlation matrices are calculated from

$$\mathbf{R}_r = E\{\mathbf{H}\mathbf{H}^\dagger\}, \tag{2.9}$$

$$\mathbf{R}_t = E\{\mathbf{H}^\dagger\mathbf{H}\}. \tag{2.10}$$

The channel correlation matrix is modeled by [20]

$$\mathbf{R}_h = \frac{1}{\sqrt{tr\{\mathbf{R}_r\}}}\mathbf{R}_t \otimes \mathbf{R}_r. \tag{2.11}$$

The beamforming input parameters assuming the Kronecker model reduce to

$$\mathbf{S}_t^{kron} = (\sqrt{\mathbf{R}_t}^T \otimes \sqrt{\mathbf{R}_t}^\dagger)\mathbf{I}_t(\sqrt{\mathbf{R}_r}^T \otimes \sqrt{\mathbf{R}_r}^\dagger), \tag{2.12}$$

$$\mathbf{S}_r^{kron} = (\sqrt{\mathbf{R}_r}^* \otimes \sqrt{\mathbf{R}_r})\mathbf{I}_r(\sqrt{\mathbf{R}_t}^* \otimes \sqrt{\mathbf{R}_t}), \tag{2.13}$$

where $\mathbf{I}_t = E\{\mathbf{H}_w^T \otimes \mathbf{H}_w^\dagger\}$ and $\mathbf{I}_r = E\{\mathbf{H}_w^* \otimes \mathbf{H}_w\}$. Under this model, the feedback complexity decreases to $2N_rN_t$. As a consequence of the simplicity, this model is widely used despite known performance prediction issues [20].

On the other hand, the Kronecker model might not be able to correctly capture the underlying structure of the channels since it holds only if the channels can be separated into two independent link ends. It has relatively limited validity and the Kronecker approximation yields better results for small array sizes [17]. It often provides significant underestimation of the capacity for indoor MIMO systems using large linear arrays.

2.4.3 Weichselberger Model

In contrast to the Kronecker model, the Weichselberger model does not divide the spatial correlation properties of the channel into separate contributions from transmitter and receiver [21]. Instead, it considers the statistical interdependence of both link ends using joint correlation properties. The Weichselberger model combines the advantages of the Kronecker model with a virtual channel representation. Specifically, it models the mutual dependence by describing the average coupling between the eigenmodes of the two link ends through a coupling matrix. It has been shown that the Weichselberger model overcomes some of the deficiencies discovered in the Kronecker model and has improved capability of modeling the spatial multipath structure of realistic MIMO channels correctly.

Under the Weichselberger model, channel matrix realizations are represented as

$$\mathbf{H}_{weichs} = \mathbf{U}_r(\tilde{\Lambda} \odot \mathbf{H}_w)\mathbf{U}_t^T, \tag{2.14}$$

where $\tilde{\Lambda}$ is the element-wise square root of the matrix Λ, $\odot$ is the matrix element-by-element product operator, and the matrices $\mathbf{U}_r$ and $\mathbf{U}_t$ respectively contain the eigenvectors of $\mathbf{R}_r$ and $\mathbf{R}_t$ from the Kronecker model.

By using the properties of the Kronecker product, we can write

$$\mathbf{S}_t^{weichs} = (\mathbf{U}_t \otimes \mathbf{U}_t^*)(\tilde{\Lambda}^T \otimes \tilde{\Lambda}) \odot \mathbf{I}_t(\mathbf{U}_r^T \otimes \mathbf{U}_r^\dagger), \tag{2.15}$$

$$\mathbf{S}_r^{weichs} = (\mathbf{U}_r^* \otimes \mathbf{U}_r)(\tilde{\Lambda}^* \otimes \tilde{\Lambda}) \odot \mathbf{I}_r(\mathbf{U}_t^\dagger \otimes \mathbf{U}_t^T). \tag{2.16}$$

The Weichselberger model requires a feedback complexity of $N_r^2 + N_t^2 + N_r N_t$.

Thus, while the Weichselberger model may still offer a simplification of the required parameters needed to generate the channel model, as compared to the full correlation analytical model, its additional complexity can make it less attractive than the Kronecker model for certain applications in system design. However, under certain transmission geometries, the Weichselberger model provides a near-perfect match to the correlation values at all interelement spacings studied[18]. In all, the Weichselberger model offers a better approximation of the full correlation, and achieves a better performance-complexity compromise than the Kronecker model.

To facilitate the development of MIMO system architectures and design of optimal signaling strategies, where creating many different channel matrix realizations for a variety of communication environments is desired, these correlation-based analytical models have been widely used. Although they might have limited validity in realistic propagation scenarios, these models have still been considered powerful tools in developing MIMO systems, underscoring the significance of the spatial correlation on MIMO system design.

2.5 Channel Wide-Sense Stationarity Violation

It is very common to estimate the spatial channel covariance by using a sample mean over a certain time period to approximate the expectation[11, 12]. The key assumption underlying this estimation method is that the channel covariance is constant over the time period. This assumption implies that the channel is a statistically wide-sense stationary process. When we use channel covariance as partial CSI to be fed back to the transmitter in a MIMO system implementation, this approximate computation of the covariance might be acceptable even though the stationarity assumption might not strictly hold. For example, in previous studies of signaling strategy design based on covariance feedback, using a sample mean to estimate the covariance matrix resulted in reasonably good and stable communication performance.

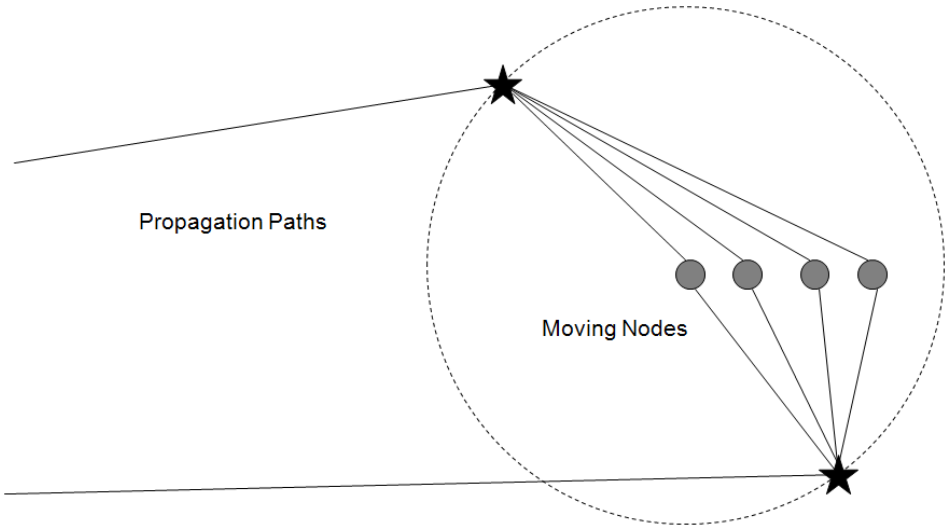

Figure 2.3: Multipath propagation angles changing with node position.

However, if we turn our focus to modeling the time evolution of the channel covariance, which represents the change of the spatial structure of the channel multipaths, we must recognize that this stationarity assumption cannot be considered to be valid. Figure 2.3 shows the situation where the wide-sense stationarity is violated. We assume that scatterers lie of a circle around a node and that the node is moving through the environment. Since the scatterers are usually relatively stable objects such as trees, buildings and furniture, the multipath angles from these scatterers to the node are changing with node position, which is clearly demonstrated in Figure 2.3. Because the channel covariance depends critically on the multipath angles, clearly the channel covariance evolves with node position as well. If the scatterers are moving objects such as cars and people, the multipath angles will also change with their locations, again leading to changes in the channel covariance. Under such circumstances, we explicitly acknowledge that the underlying channel is not a wide-sense stationary process, and we desire to characterize the evolution of the channel covariance by a model.

The challenge with this acknowledgement, however, is that it now becomes difficult even to define the spatial covariance. Specifically, when estimating the covariance matrices from the data measured over a range of positions in a time sequence, the spatial window or the length of the time period over which the expectation should be performed is undetermined.

For example, if the window is too small, the covariance will vary rapidly which violates the nature of the covariance and thus makes the reduction in frequency of feedback unrealistic in practical precoding strategies, and if it is too large, it will not represent the structure describing the spatial channel characteristics, which is essential for MIMO channel modeling and performance analysis. Therefore, the remainder of this thesis is devoted to studying the behavior of the channel spatial covariance in time-varying environments and to understanding how the covariance should be estimated.

Chapter 3

Analytical Covariance Model and Correlation Matrix Distance

Because CSI depends on the interference of multiple propagating wave components, the channel coefficients and their associated eigenstructure change quickly with node position [22]. This makes it difficult to capture the useful correlative information for node separations and identify the similarities between channel matrices of adjacent nodes for a multi-user MIMO system. In contrast, channel covariance depends on the spatial structure of the multipaths, such as angles of departure and arrival and path gains, which varies more slowly with node separation. Therefore it is interesting to investigate the nature of the channel covariance as a function of node position and thus use that information in channel modeling.

However, when discussing the evolution of the channel covariance, we cannot assume the channel is a wide-sense stationary process and therefore cannot easily estimate the covariance by averaging over a window. It is best to construct an analytical model to assist our investigation. This chapter describes the analytical approach and its application given a geometrical propagation model and introduces a metric for quantifying the non-stationarity of the channel.

3.1 Analytical Covariance Model

The closed-form model that allows estimation of the full MIMO covariance is based on knowledge of the power angular spectrum (PAS) of the channel and the antenna radiation patterns. Let

$$\beta(\Omega_r, \Omega_t) = \begin{bmatrix} \beta_{\theta\theta}(\Omega_r, \Omega_t) & \beta_{\theta\phi}(\Omega_r, \Omega_t) \\ \beta_{\phi\theta}(\Omega_r, \Omega_t) & \beta_{\phi\phi}(\Omega_r, \Omega_t) \end{bmatrix}, \tag{3.1}$$

where each matrix entry $\beta_{uv}(\Omega_r, \Omega_t)$ represents the complex gain function for a multipath component departing at the angle Ω_t with polarization $v \in [\theta, \phi]$ and arriving at the angle Ω_r with polarization $u \in [\theta, \phi]$. Then, the element of the channel matrix can be expressed using the superposition integral

$$H_{mn} = \int \int \mathbf{e}_{r,m}^T(\Omega_r)\beta(\Omega_r, \Omega_t)\mathbf{e}_{t,n}(\Omega_t)d\Omega_r d\Omega_t, \tag{3.2}$$

where

$$\mathbf{e}_{r,m}(\Omega_r) = [e_{r\theta,m}, e_{r\phi,m}]^T \tag{3.3}$$

indicates the vector radiation pattern of the mth receive antenna and $\mathbf{e}_{t,n}(\Omega_t)$ has a similar definition for the nth transmit antenna.

Our goal is to determine the covariance consisting of terms $R_{mn,pq} = E\{H_{mn}H_{pq}^*\}$. If we let $\mathbf{b}(\Omega_r, \Omega_t) = vec\{\beta(\Omega_r, \Omega_t)\}$ and make the common assumption that the field arriving (or departing) from one angle is uncorrelated with that arriving (or departing) from another, we obtain

$$E\{\mathbf{b}(\Omega_r, \Omega_t)\mathbf{b}(\Omega_r', \Omega_t')^\dagger\} = \mathbf{B}(\Omega_r, \Omega_t)\delta(\Omega_r - \Omega_r')\delta(\Omega_t - \Omega_t'), \tag{3.4}$$

where

$$\mathbf{B}(\Omega_r, \Omega_t) = E\{\mathbf{b}(\Omega_r, \Omega_t)\mathbf{b}^\dagger(\Omega_r, \Omega_t)\}. \tag{3.5}$$

Then defining $\mathbf{e}_{mn} = \mathbf{e}_{r,m} \otimes \mathbf{e}_{t,n}$ allows us to write the desired element of the covariance matrix as

$$R_{mn,pq} = \int \int \mathbf{e}_{mn}^T(\Omega_r, \Omega_t)\mathbf{B}(\Omega_r, \Omega_t)\mathbf{e}_{pq}^*(\Omega_r, \Omega_t)d\Omega_r d\Omega_t. \tag{3.6}$$

The resulting covariance depends on the expectation used to construct $\mathbf{B}(\Omega_r, \Omega_t)$. For example, consider propagation in a single electromagnetic polarization such that all functions in the integrand of Equation (3.2) are scalars. If we assume the multipath propagation can be modeled as a set of discrete plane wave components, with the lth component defined

by the angle of departure $\Omega_{t,l}$, the angle of arrival $\Omega_{r,l}$, and the complex gain β_l, then one possible form of Equation (3.6) is

$$R_{mn,pq} = \sum_l |\beta_l|^2 e_{r,m}(\Omega_{r,l}) e_{t,n}(\Omega_{t,l}) e^*_{r,p}(\Omega_{r,l}) e^*_{t,q}(\Omega_{t,l}). \tag{3.7}$$

This implies that for each multipath component, the single element of $\mathbf{B}$ is $|\beta_l|^2$, indicating that the phase of the complex gain β_l represents the random variable over which the expectation is taken. If the magnitude of β_l is also assumed to vary, then the coefficient $|\beta_l|^2$ in Equation (3.7) should be replaced by the variance of this random variable.

3.2 Correlation Matrix Distance

Before we utilize the analytical approach to investigate the evolution property of the channel covariance, we introduce a metric for characterizing the spatial non-stationarity of the covariance. Through this useful metric we can explore the evolution of the channel covariance as a function of position.

The metric we choose to use in this study is the MIMO correlation matrix distance (CMD)[23], which measures the change in correlation matrices estimated at different times (or locations), to characterize how significantly the spatial structure of the channel has changed. Assume the $n \times 1$ time-variant signal vector $\mathbf{x}(t)$ to be a zero-mean stochastic vector process, where the element correlations are described by the time-dependent element-correlation matrix

$$\mathbf{R(t)} = E\{\mathbf{x}(t)\mathbf{x}(t)^H\}. \tag{3.8}$$

We take the correlation matrix for $t = t_1$ and $t = t_2$ and compute their inner product as

$$\langle \mathbf{R}(t_1)\mathbf{R}(t_2) \rangle = tr\{\mathbf{R}(t_1)\mathbf{R}(t_2)\} \leqslant \|\mathbf{R}(t_1)\|_F \|\mathbf{R}(t_2)\|_F, \tag{3.9}$$

where $tr\{\cdot\}$ is the trace operator and $\|\cdot\|_F$ denotes the Frobenius norm.

The *correlation matrix distance* (CMD) can then be defined as

$$d_{corr}(\mathbf{R}(t_1), \mathbf{R}(t_2)) = 1 - \frac{tr\{\mathbf{R}(t_1)\mathbf{R}(t_2)\}}{\|\mathbf{R}(t_1)\|_F \|\mathbf{R}(t_2)\|_F} \in [0, 1], \tag{3.10}$$

based on the inner product. Note that the correlation matrix distance becomes zero for equal correlation matrices and has a maximum value of unity.

This definition was reformulated in [24] as the inner product between the vectorized correlation matrices, or

$$d_{corr}(\mathbf{R}_1, \mathbf{R}_2) = 1 - \frac{\langle vec\{\mathbf{R}_1\}, vec\{\mathbf{R}_2\}\rangle}{\|vec\{\mathbf{R}_1\}\|_F \|vec\{\mathbf{R}_2\}\|_F}, \tag{3.11}$$

where $\mathbf{R}(t_1)$ and $\mathbf{R}(t_2)$ have been written as $\mathbf{R}_1$ and $\mathbf{R}_2$ respectively, for the purpose of simplicity. This formulation makes it clear that the CMD measures the 'orthogonality' between the considered correlation matrices in the $n \times n$ dimensional space. This concept is reinforced using an eigenvalue analysis. Specifically, the product of the correlation matrices can be expressed as

$$\mathbf{R}_1\mathbf{R}_2 = \mathbf{U}_1\Lambda_1\mathbf{U}_1^\dagger\mathbf{U}_2\Lambda_2\mathbf{U}_2^\dagger = \mathbf{U}_1\mathbf{D}\mathbf{U}_2^\dagger, \tag{3.12}$$

where

$$(\mathbf{D})_{i,j} = \mathbf{u}_{(1),i}^\dagger \mathbf{u}_{(2),j} \lambda_{(1),i}\lambda_{(2),j} \tag{3.13}$$

denotes element (i, j) of $\mathbf{D}$, $\mathbf{u}_{(1),i}$ and $\mathbf{u}_{(2),j}$ respectively indicates the ith and jth column of $\mathbf{U}_1$ and $\mathbf{U}_2$, and $\lambda_{(1),i}$ and $\lambda_{(2),j}$ are the corresponding eigenvalues. Equation (3.12) implies that $\mathbf{D}$ becomes zero if for every pair of eigenvectors either $\mathbf{u}_{(1),i}$ and $\mathbf{u}_{(2),j}$ are orthogonal or either $\lambda_{(1),i}$ or $\lambda_{(2),j}$ is zero. If $\mathbf{D}$ becomes a zero matrix, $tr\{\mathbf{R}_1\mathbf{R}_2\}$ also becomes zero and therefore the CMD has a value of one. However, the more the signal spaces of $\mathbf{R}_1$ and $\mathbf{R}_2$ overlap, the higher the trace of the product of $\mathbf{R}_1$ and $\mathbf{R}_2$ becomes, and thus the CMD decreases.

Due to its nature of measuring the 'orthogonality', the CMD can be considered as a useful tool to evaluate whether the spatial structure and therefore the channel statistics have changed by a substantial amount. Some indoor and outdoor-to-indoor measurements

have been reported in the literature[24, 25]. The CMD curves as functions of position or separation have been calculated, which show some very interesting results. First, the results suggest that new multi-user MIMO channel models describing the spatial characteristics of channels of different users could be based on the evolution of the covariance, and that appropriate scheduling and precoding algorithms can be designed to minimize the spatial interference. Futhermore, the results show that high values of the CMD corresponding to substantial changes in the spatial structure of the channel are an indication of a significant performance degradation of the transmission signaling strategy due to the non-stationarity of the channel [24]. This suggests that the CMD is a meaningful measure to assess the stationarity of the channel.

This previous work, however, uses measured data under some specific environments, and thus the conclusions drawn from them might not be valid in other physical circumstances or in general. Moreover, the evolution behavior of the channel covariance versus node location have not been investigated in the previous work, even though some observations of the general range of the CMD have been made. Motivated by these studies, we focus on the varying behavior of the channel covariance as a function of node position.

3.3 Example simulation Using the Analytical model and CMD

Let us consider a two-ring propagation model as the basis of our example simulation to find some interesting results about the evolution behavior of the channels as function of node location by applying the analytical approach and the CMD metric.

3.3.1 Two-Ring Propagation Model

A simple two-ring propagation model is shown in Figure 3.1, where each propagation path is confined to a single plane and a few scatterers are located on two circles: one around the transmitter and another around the receiver. Each propagation path from the transmitter to the receiver passes through one scatterer on each circle. The angular location of each scatterer is defined as a uniformly distributed random variable, and the complex gain of each path is modeled as a circularly-symmetric zero-mean unit-variance complex Gaussian random variable. An antenna array is placed in the center of each circle, one as

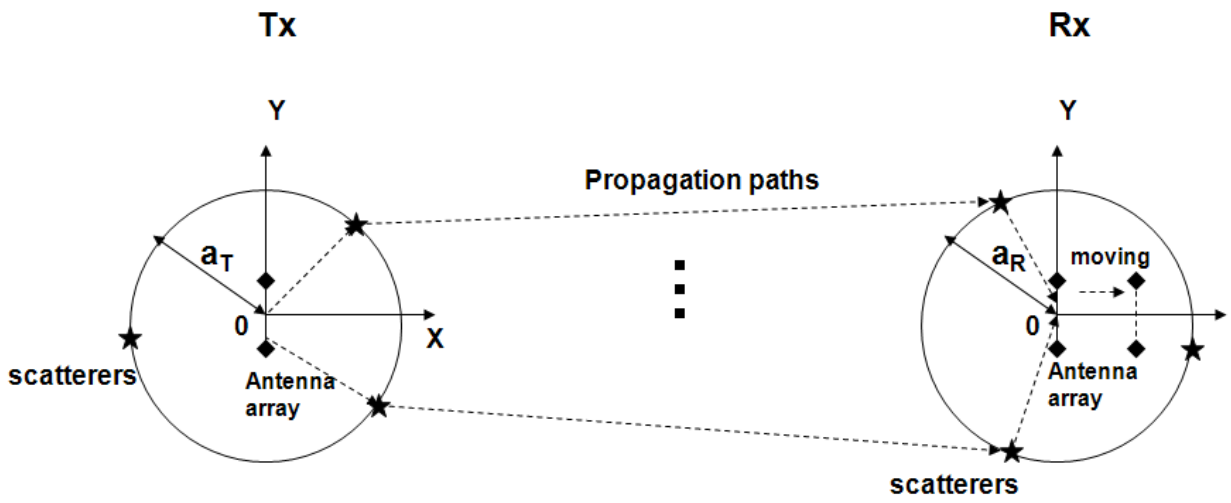

Figure 3.1: The geometry of a two-ring propagation model assuming a two-dimension path plane.

the transmitter and one as the receiver. Each antenna is a uniform linear array with 8 omnidirectional elements oriented along the y-axis with $\lambda/2$ element spacing, where λ is the free-space wavelength.

In the example simulation, we assume that the receiver antenna array moves along the x-axis from the center of the circle (origin of the xy-coordinate) to a location of $x_r = a_R/3$ where the CMD of the channel covariance reaches the first peak value, x_r indicates the x-coordinate of the receiver position in the receiver coordinate frame, and a_R indicates the radius of the scatterer circle at the receiver. Samples of the channel are taken at an interval of $1/25$ λ (of receiver motion), and at each location the covariance may be computed using Equation (3.7). Denoting the covariance as a function of receiver location as $\mathbf{R}(x_r)$, we may calculate the CMD as

$$\mathbf{CMD}(x_r) = 1 - \frac{tr\{\mathbf{R}(0)\mathbf{R}(x_r)\}}{\|\mathbf{R}(0)\|_F \|\mathbf{R}(x_r)\|_F}. \tag{3.14}$$

As described in the last section, CMD provides a measure of similarity between the covariance at the initial point and that at a different position, with $CMD = 0$ implying the matrices are the same and $CMD = 1$ indicating that they are unrelated.

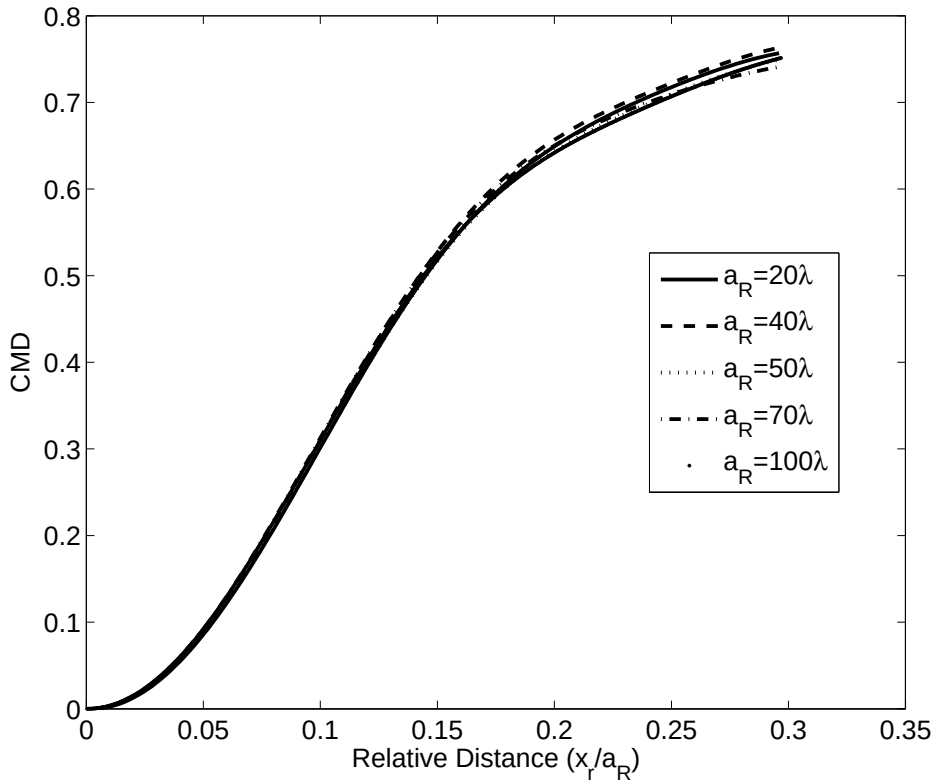

Figure 3.2: Average CMD as a function of normalized node displacement assuming a 8×8 MIMO system with propagation characterized by a two-ring model with 3 propagation paths.

3.3.2 Simulation Results and Implications

The simulation uses 500 different channel realizations for five different values of a_R and 3 multipath components (scatterers). In each realization, the channel covariance matrix at each receiver location indicated by x_r has been calculated and the CMD as a function of x_r has been computed by Equation (3.14). The resulting CMD curves are shown in Figure 3.2, where the displacement is normalized by the circle radius a_R. This normalization is intuitive because the normalized distance controls the rate of change of the angles of arrival which in turn controls the covariance structure. The results reveal that the evolution behavior of the covariance as a function of normalized distance for different values of a_R are similar, meaning that it is the relative displacement, not the absolute displacement, that affects the change of the covariance. Furthermore, the results demonstrate that the covariance matrices

at two different locations maintain a strong relationship for a relative distance up to 15% of a_R (which represents the average distance to the scatterers).

Extending the results to a usable MIMO model requires additional work. However, one can envision a simple stochastic MIMO model where the covariance matrices themselves are random variables, with the matrix at one location correlated with that at another according to the CMD metric shown in Figure 3.2. Channel matrices could then be realized based on this correlation.

Chapter 4

Methods of Determining Window Size for Covariance Estimation

The analytical framework in Chapter 3 provides a basis for understanding the dependence of the covariance on the spatial channel properties. Here, we extend this understanding to determining the appropriate window size that should be used for covariance estimation from channel realizations.

4.1 Sensitivity of Covariance Change Rate to Window Size Used to estimate Covariance

Our objective is to use the CMD metric to understand the impact of window size on the covariance behavior. In our analytical formulation of the covariance, we have already obtained the expression of each element of the channel matrix, written in Equation (3.2), which may be further used to estimate the covariance through Equation (2.3), where a sample mean over a window will be used to estimate the expectation. In the two-ring propagation model, where the geometry is determined and a distribution of scatterers in the environment is assumed, the generation of channel matrices then becomes a ray tracing problem. Each entry H_{mn} in the channel matrix may be computed by

$$H_{mn} = \sum_{l=1}^{L} \beta_l e^{jk(x_m cos\phi_{Rl} + y_m sin\phi_{Rl})} e^{jk(x_n cos\phi_{Tl} + y_n sin\phi_{Tl})}, \tag{4.1}$$

where m and n index the receive and transmit antennas respectively, $k = \frac{2\pi}{\lambda}$ is the wave number, l indicates the index of each propagation path to the receiver and L is the total number of the paths, β_l is the complex gain for each scatterer (path), x_m and y_m represent the x-coordinate and y-coordinate of the mth element of the receive array respectively, x_n and y_n represent the x-coordinate and y-coordinate of the nth element of the transmit array

respectively, and ϕ_{Rl} means the angle of arrival (AOA) of the lth path while ϕ_{Tl} implies the angle of departure (AOD) of the lth path.

The two-ring propagation model is constructed as outlined in Chapter 3 for the simulations. Samples of the channel are taken at an interval of $\lambda/10$ in receiver motion. For each sample, a channel realization $\mathbf{H}$ is computed through Equation (4.1). The resulting sequence of channel matrices $\mathbf{H}$ may be generated and the covariance corresponding to the kth sample point, with definition of $\mathbf{R}^{(k)} = E\{vec\{\mathbf{H}^{(k)}\}vec\{\mathbf{H}^{(k)}\}^{\dagger}\}$, may be estimated from the sequence of $\mathbf{H}$ by

$$\mathbf{R}_{est}^{(k)} = \frac{1}{N}\sum_{n=k}^{N+k-1} vec\{\mathbf{H}^{(n)}\}vec\{\mathbf{H}^{(n)}\}^{\dagger}, \tag{4.2}$$

where the sample mean over a window of size N is used to approximate the expectation $E\{\cdot\}$ and $\mathbf{H}^{(n)}$ indicates the channel matrix at sample n.

The CMD as a function of receiver displacement generated from the analytical approach introduced in Chapter 3 as well as from the estimated covariance for 5 different window sizes are provided in Figure 4.1. Because the CMD represents the difference between two covariance matrices, the CMD curve as a function of displacement indicates the variation of the channel covariance with node position. These results demonstrate that the rate of change of the covariance is sensitive to the window size used during covariance estimation. The curves also show that the rate of change can deviate significantly from that predicted using the analytical model.

The fact demonstrated in Figure 4.1 that the rate of change of the channel covariance is sensitive to the window size used to estimate the expectation may be explained from the non-stationarity of the channel. Since the true channel covariance varies with node location, the channel cannot be assumed to be a wide-sense stationary process. When we estimate the channel covariance using an average over a spatial window, we consider that within the spatial window the channel covariance remains constant which means the channel is assumed to be wide-sense stationary within the window. The difficulty, therefore, lies in determining the appropriate window size. If the window is too small, the estimated channel covariance

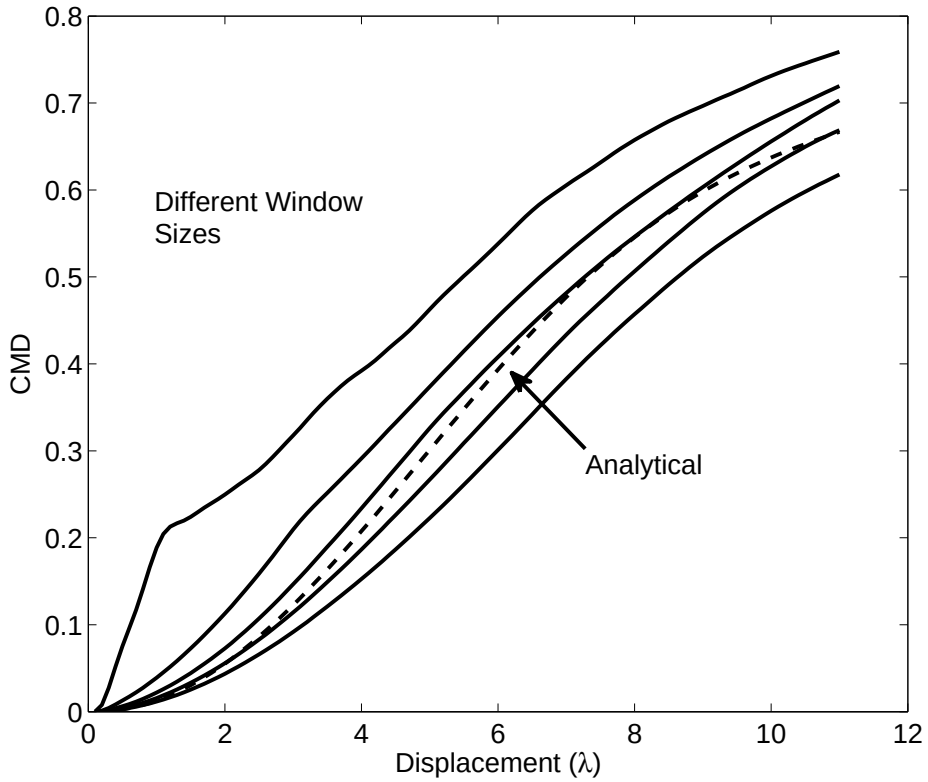

Figure 4.1: Average CMD of covariance generated by analytical model and estimated from channel realizations through different window sizes for a scatterer circle of radius 10 λ.

will change too rapidly. If the window is too large, the estimated channel covariance will not represent accurately the spatial structure of the channel.

Figure 4.2 shows the average slope of the CMD curve as a function of the size of the estimation window. The average slope of the CMD computed from the analytical model is about 0.062. However, the average slope of the CMD computed from the covariance estimated by averaging over a spatial window varies significantly. For this problem, the slope from the estimated covariance matches that obtained from the analytical solution at a window size of approximately 7 λ.

4.2 Method by Quantifying Average Variation of Covariance

Motivated by the observations drawn from Figures 4.1 and 4.2, we derive a method for determining the appropriate window size used to estimate the channel covariance by

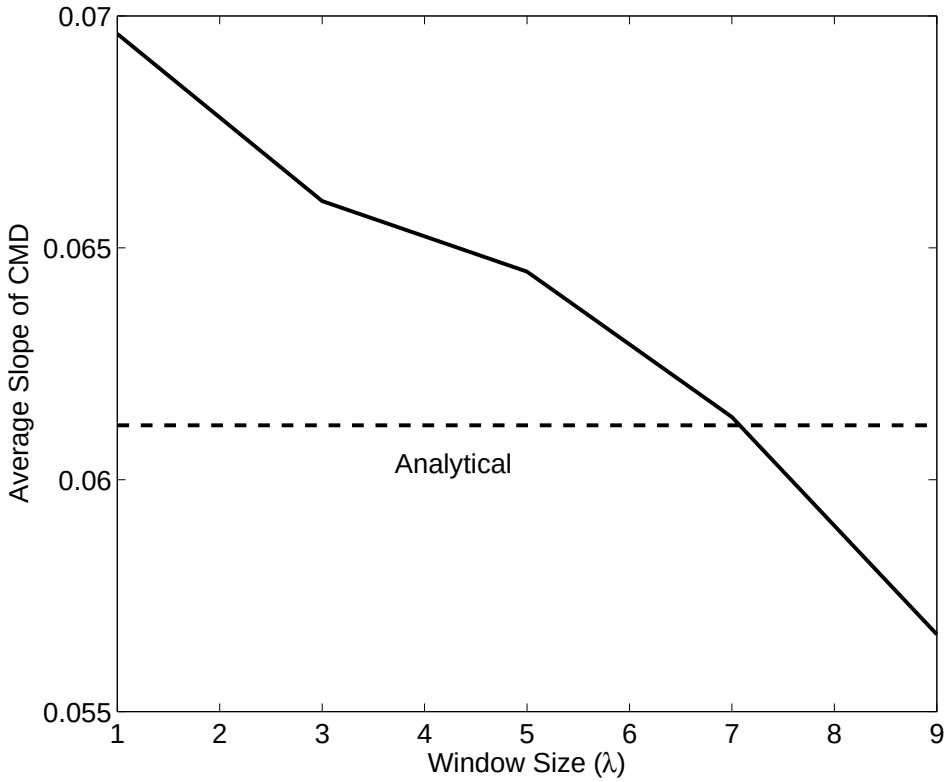

Figure 4.2: Average slope of CMD of covariance generated by analytical model and estimated from channel realizations through different window sizes of 1, 3, 5, 7 and 9 λ.

quantifying the average slope of the covariance. Approximating the magnitude of the first derivative of the CMD at the kth sample as

$$f(k) = |\frac{\Delta CMD}{\Delta x}| \approx |\frac{CMD(x(k+1)) - CMD(x(k))}{x(k+1) - x(k)}|, \tag{4.3}$$

we may compute the average variation of the covariance as

$$\chi = \frac{1}{N} \sum_{k=1}^{N} f(k), \tag{4.4}$$

where k is the position index, x represents the position at which the $CMD(x)$ between covariance matrices $\mathbf{R}(0)$ and $\mathbf{R}(x)$ is computed, and N indicates the total number of position indices.

Given this definition of χ, we now use it to determine the window size for covariance estimation. Specifically, we compute χ using the analytical model as well as using the sample mean of the channel matrices over different window sizes. We then choose the window size at which the values of χ obtained using the two methods are approximately equal. In the next chapter, we will use simulation results to show the performance of this method.

4.3 Method by Finding Minimum Mean Square Error Between CMDs

In statistics and signal processing, a minimum mean square error (MMSE) estimator describes an approach that minimizes the mean square error (MSE) between the estimated and true values of the quantity of interest. The error in such an analysis is the amount by which the estimated value differs from the true value. For example, if X is the quantity being estimated and $\hat{X}$ is the estimated value, then the MSE can be defined by

$$MSE = E\{(\hat{X} - X)^2\}. \tag{4.5}$$

The MMSE estimator is then defined as the estimator achieving minimal MSE.

Such an approach can be used in our quest to identify the optimal window size for covariance estimation. Specifically, we define the optimal window size as the one that minimizes the MSE between the CMD obtained from the analytical solution and that obtained from the channel estimates. Mathematically, this means finding the window size that minimizes the error function

$$MSE_{CMD} \approx \frac{1}{N} \sum_{k=1}^{N} |CMD_{est}(k) - CMD(k)|^2, \tag{4.6}$$

where CMD_{est} indicates the CMD curve of the covariance estimated from channel realizations and k is the index. Alternatively, we can use the root mean square error (RMSE), which means finding the window that minimizes the error function

$$RMSE_{CMD} \approx \sqrt{\frac{1}{N} \sum_{k=1}^{N} |CMD_{est}(k) - CMD(k)|^2}. \tag{4.7}$$

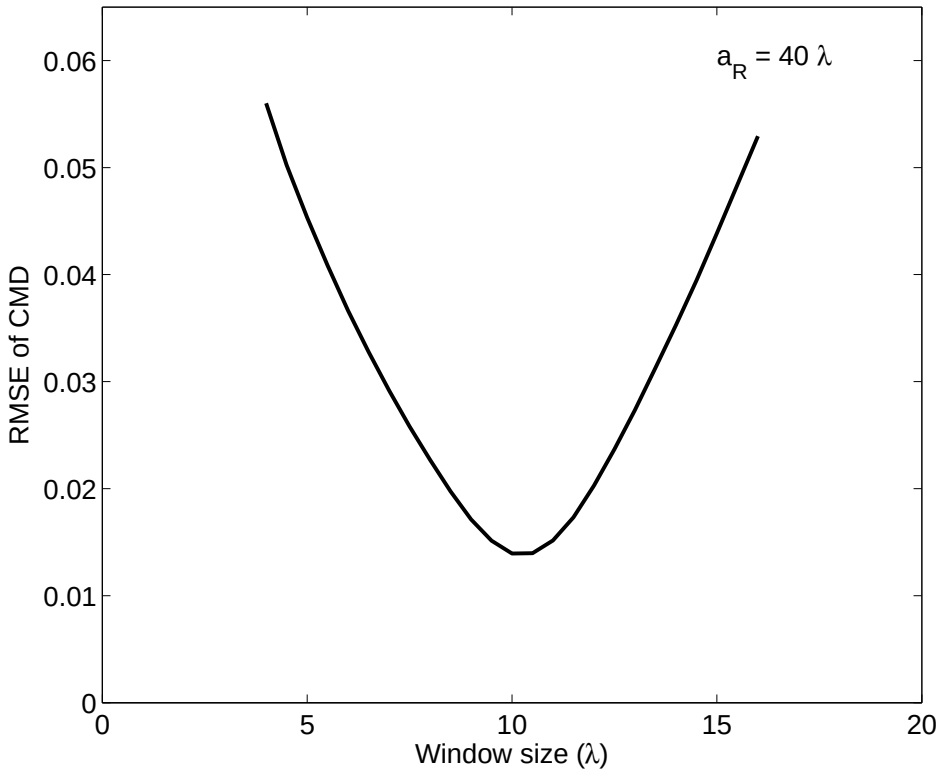

Figure 4.3: Root mean square error of the CMD for the two covariance computation methods as a function of the window size used to obtain the estimated covariance.

Figure 4.3 plots the RMSE as a function of the window size using the simulations detailed in Figure 4.2 for a circle of radius $a_R = 40\lambda$. It is clearly shown in this figure that there is an 'optimal' window size at which the CMD of the estimated covariance is closest to that obtained using the covariance computed using the analytical solution.

4.4 Summary of the Chapter

The approaches for determining the appropriate window size are summarized in the flowcharts shown in Figures 4.4 and 4.5. In the following chapter, these two methods will be applied to data from different simulations to analyze their performance and to obtain an improved understanding of the behavior of the spatial covariance matrices.

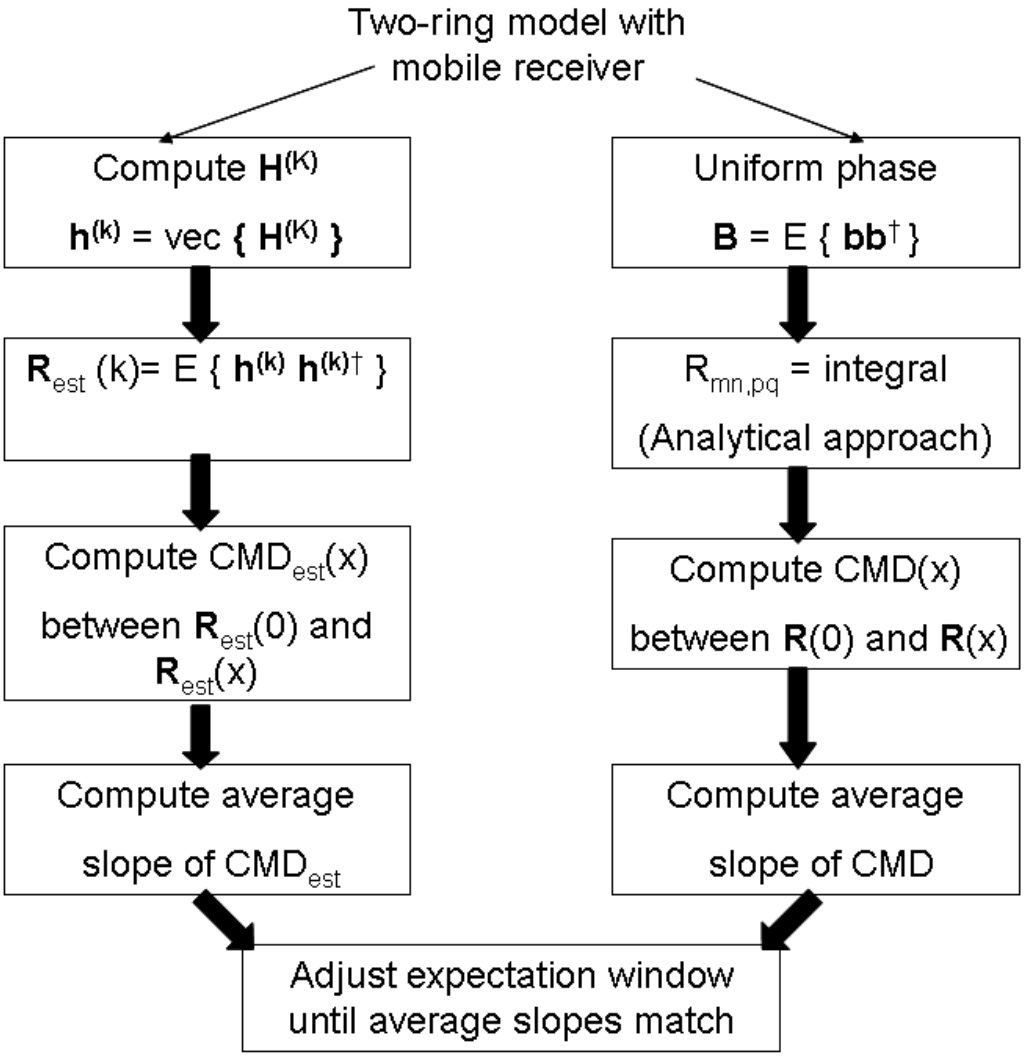

Figure 4.4: Flowchart showing the method for determining the expectation window size by quantifying average variation of the channel covariance.

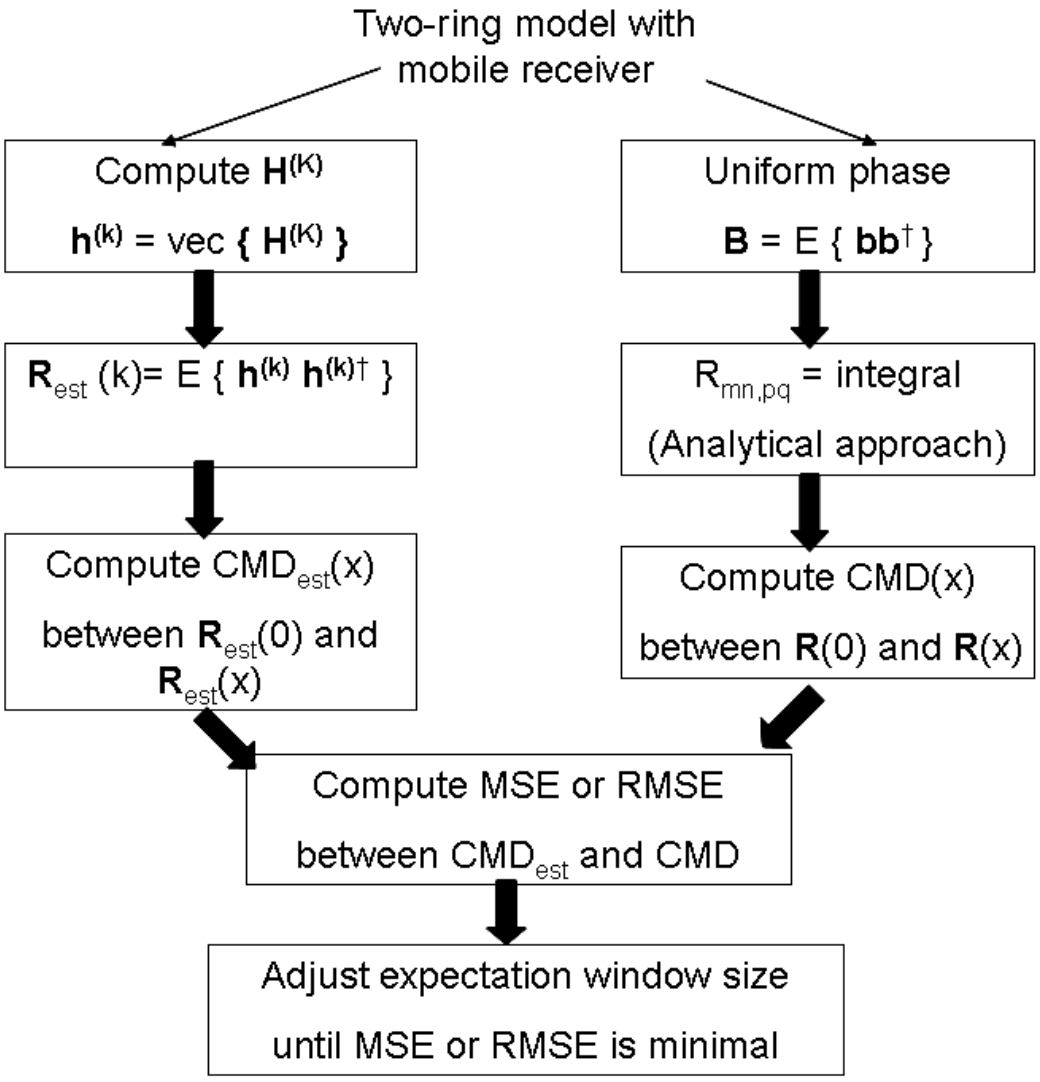

Figure 4.5: Flowchart showing the method for determining the expectation window size by finding the MMSE or minimum RMSE between CMD and estimated CMD curves.

Chapter 5

Simulations Based on Two-Ring Model and Ray-Tracing Data

Given the methods outlined in Chapter 4 for determining an appropriate window size for covariance estimation, we turn attention to application of the methods to simulated propagation data. The goal is to explore the impact of different parameters regarding the propagation environment on the behavior of the covariance and on the window size used for its estimation. Ultimately, the objective is to be able to use this understanding to assist in the estimation of the covariance from measured data, which would be a practical outcome of the concepts in this research.

5.1 Simulations Based on Two-Ring Propagation Model

Again, we consider the simple two-ring propagation model discussed in Chapter 3, where each multipath component is confined to a single plane and scatters from one object on a circle around the transmitter and another on a circle around receiver. The angular position of each scatterer on the circle is modeled as a uniformly distributed random variable, and the complex gain of each path is modeled as a circularly-symmetric zero-mean unit-variance complex Gaussian random variable. The antennas are 8-element uniform linear arrays of omnidirectional elements along the x-axis with $\lambda/2$ element spacing, where λ is the free-space wavelength. The transmit antenna array remains fixed at the circle center while the receive antenna array moves over the range $0 \leq x_r \leq a_R$, where x_r is the x-coordinate in the receiver coordinate frame and a_R is the circle radius.

All results represent averages obtained over 1000 random channel realizations. The covariance as a function of the receiver position computed using Equation (3.7) is referred to as the *analytical* value, while that obtained by computing $\mathbf{H}$ from Equation (3.2) (or more specifically from Equation (4.1)) at each position and estimating the covariance from

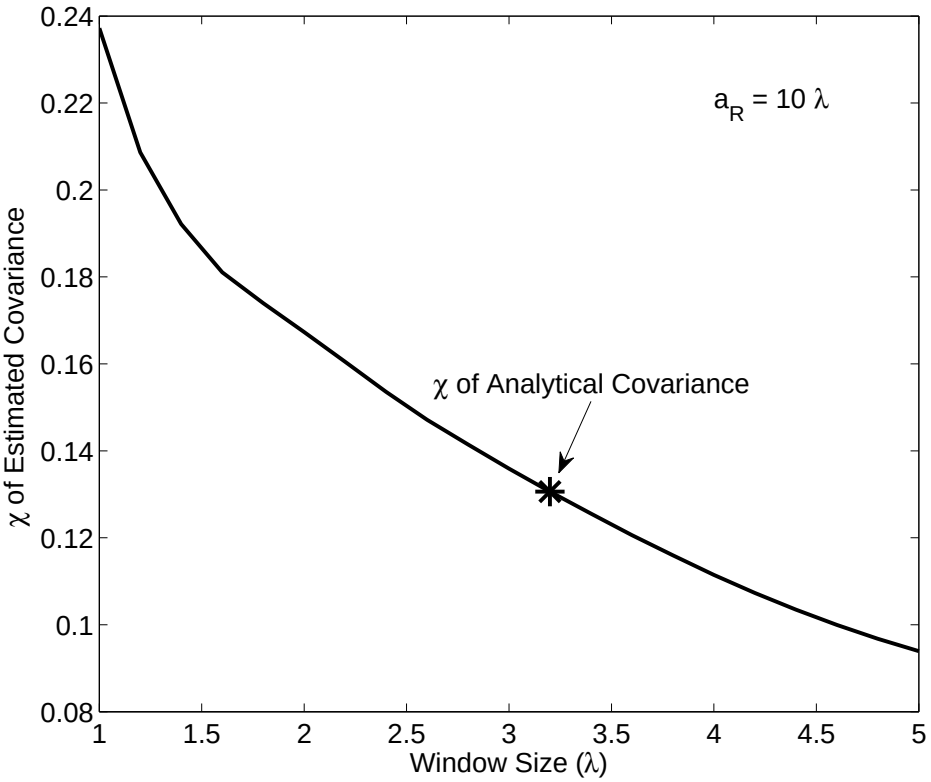

Figure 5.1: The average variation χ of estimated covariance as a function of corresponding window size matching the χ of analytical covariance to determine a window size.

Equation (4.2) by approximating the expectation with a sample mean over a window in the receiver displacement is designated as the *estimated* value. The CMD is computed from Equation (3.14) as a measure of the relative change in the covariance as a function of receiver position.

5.1.1 CMD Agreement at Different Circle Radii

Given the CMD as a function of receiver position, we compute the average slope of CMD, or the average variation of covariance χ from Equation (4.4). We define $\chi_{est}(ws)$ as the average variation of estimated covariance, where ws represents the window size used to estimate the covariance. We also denote the average variation of the analytical covariance by χ_a. We then find the window size ws such that $\chi_{est}(ws) \approx \chi_a$.

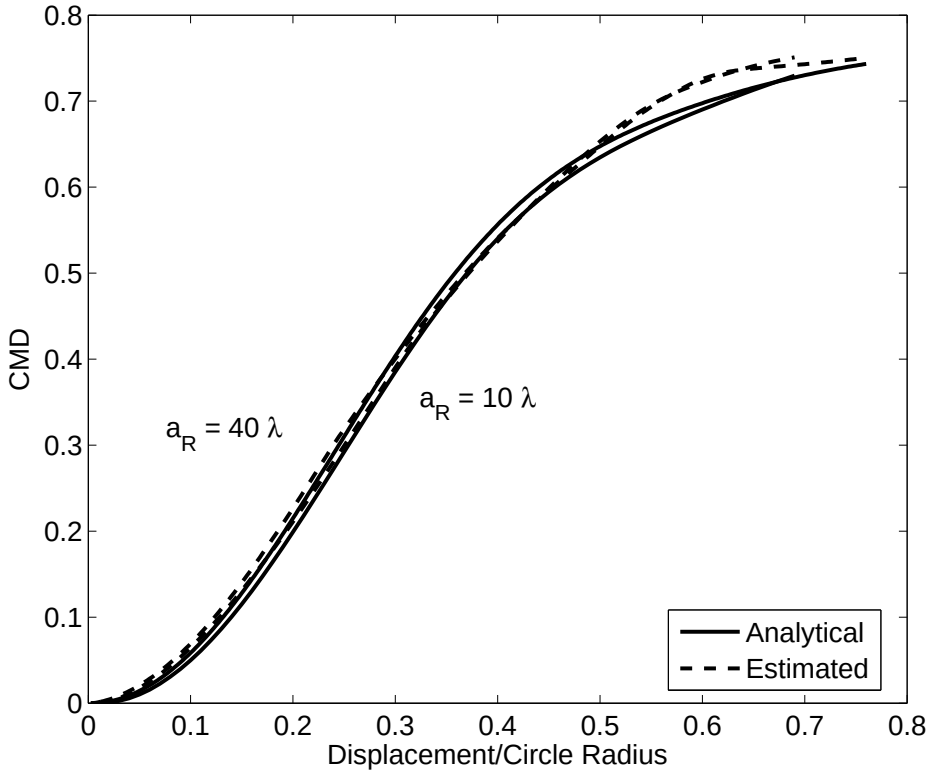

Figure 5.2: Average CMD for two different values of a_R as a function of receiver displacement, with the estimated covariance obtained using the optimal window size.

Figure 5.1 plots $\chi_{est}(ws)$ as a function of the window size ws, explicitly showing that value χ_a obtained using the analytical solution. For this simulation, the scatterer circle has a radius of $a_R = 10\lambda$ and three scatterers are used on each circle. These results show that the optimal window size for this scenario is around 3.1λ.

Figure 5.2 shows the variation in CMD as a function of receiver displacement for two different values of a_R for both the analytical and estimated covariance, where the window size for the covariance estimation is obtained using the procedure of matching the average slope. The displacement variable is normalized by the circle radius a_R, allowing inclusion of the results for different circle radii of $a_R = 10\lambda$ and $a_R = 40\lambda$. These results reveal that with the correct window size, the estimated covariance has an average rate of change that matches that predicted by the analytical model.

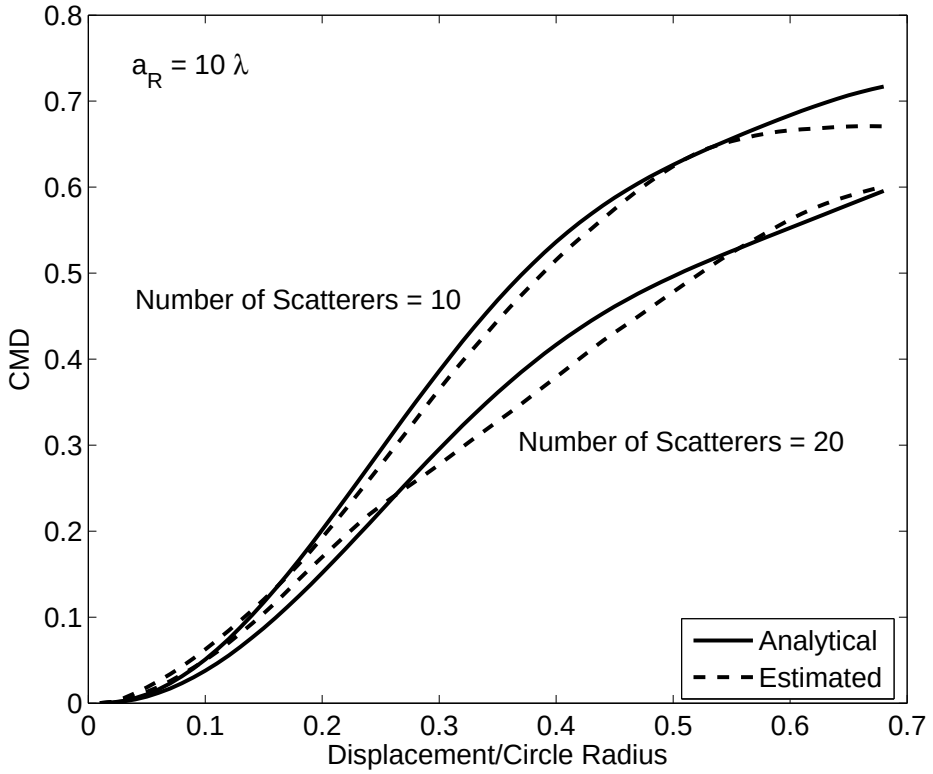

Figure 5.3: Average CMD for two different numbers of scatterers as a function of displacement with $a_R = 10\lambda$.

5.1.2 CMD Agreement Regarding Different Numbers of Propagation Paths

The number of objects on the circle around the transmit and receive antenna arrays determines the number of propagation paths used in the two-ring model. We therefore consider this multipath richness as a second parameter of interest and explore its impact on the optimal window size.

We respectively assume 10 and 20 scatterers on the circles for a circle radius $a_R = 10\lambda$. For each case, the optimal window sizes obtained by averaging over 1000 channel realizations and by matching $\chi_{est}(ws)$ to χ_a are 5λ and 6.2λ, respectively. Figure 5.3 plots and compares the CMD from the estimated covariance using the optimal window size and the analytical covariance. This result shows that the number of propagation paths significantly impacts the rate of change of the covariance as well as the optimal window size.

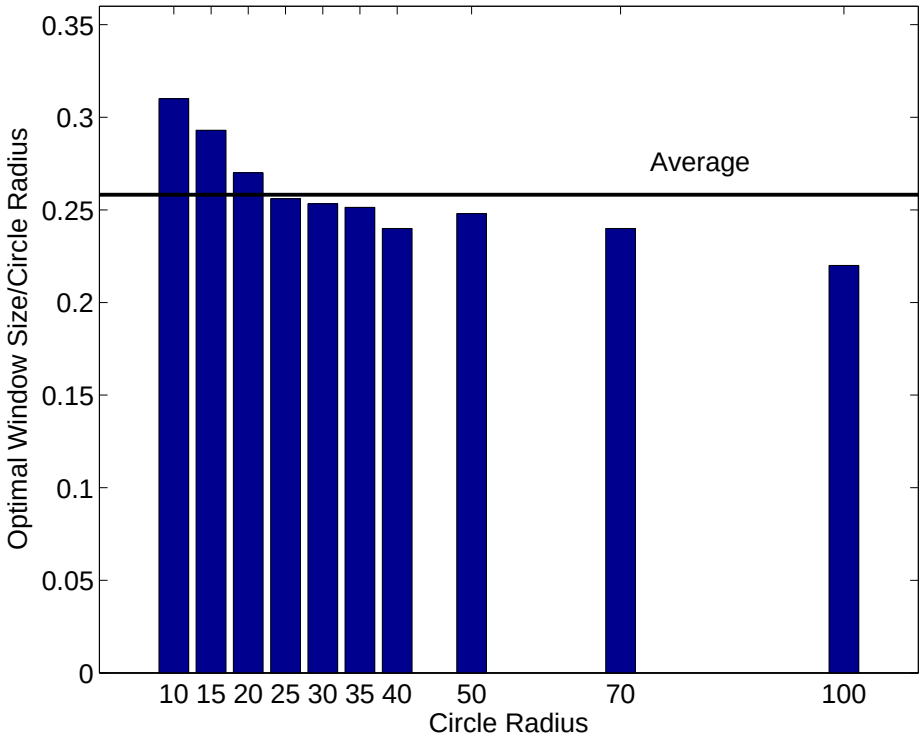

Figure 5.4: Optimal window size normalized by the circle radius a_R as a function of a_R as well as the average value.

5.1.3 Impact of Environment on Window Size

The prior results demonstrate that circle radius, or more practically the average distance to the scatterers, as well as the multipath richness both describe the multipath spatial structure and therefore impact the covariance behavior and its estimation. Additional analysis of this impact can lead to improved understanding regarding covariance estimation.

Figure 5.4 shows the optimal window size normalized by the circle radius a_R as a function of a_R. While there is some variation in this value, the results for all radii are similar, with the average normalized window size being 0.258. It is noteworthy that when the scatterers are closer to the receiver ($a_R = 10\lambda$), a larger window relative to the circle radius is required. This is likely due to the fact that for this small radius, more displacement is required to approximate a uniform distribution of the multipath phases. When the scatterers

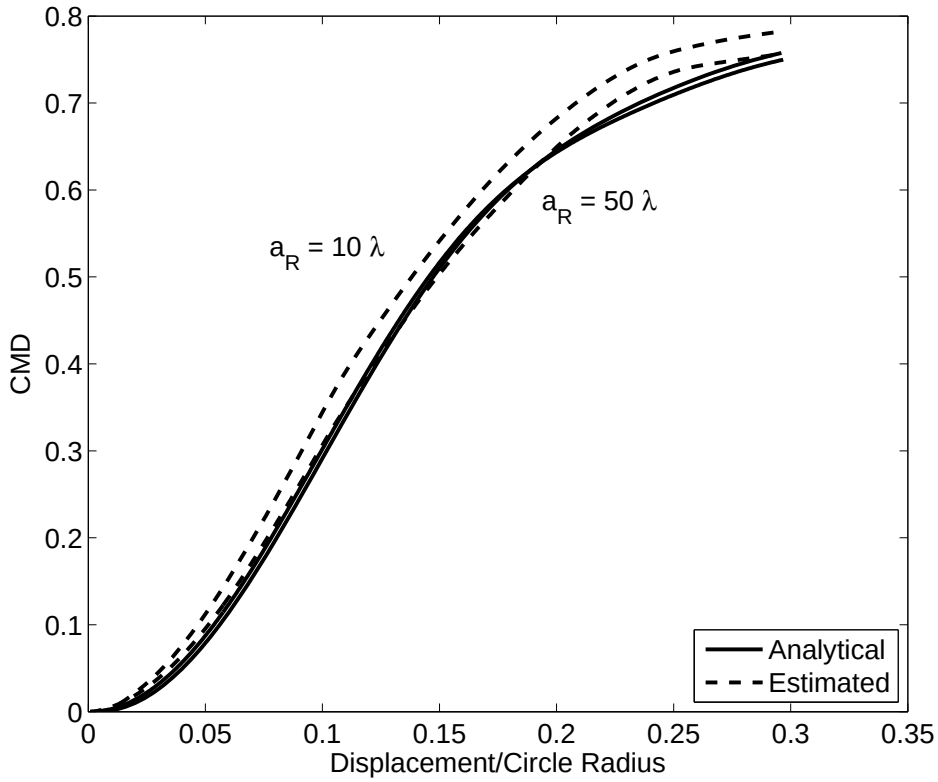

Figure 5.5: Average CMD for two different values of a_R as a function of receiver displacement, with the estimated covariance obtained using the average window size.

are further from the receiver, the displacement required can be smaller to achieve this uniform phase distribution.

We next use the average optimal window size of $0.258a_R$ (as opposed to the optimal window size for each value of a_R) to estimate the covariance from the observed channels and compute the CMD for several different values of a_R. For each value of a_R, the mean squared error (MSE) is computed between the CMD using this average window size and that using the optimal window size. Table 5.1 lists the MSE for each value of a_R. The results of CMD agreement for the two cases of $a_R = 10\lambda$ and 50λ are shown in Figure 5.5.

These results reveal that while this produces larger error in the CMD for smaller circles such as $a_R = 10\lambda$, it still represents a reasonable representation of the covariance variation. These results also suggests that if we have an estimate of the average distance between scatterers and the communication node, we should compute the covariance over a

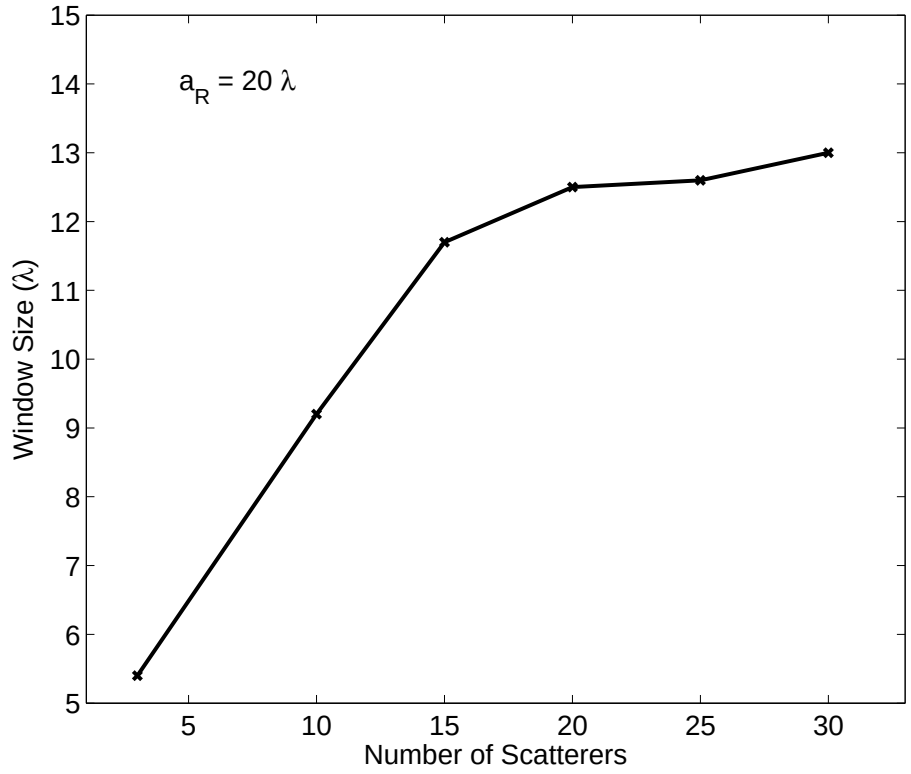

Figure 5.6: Optimal window size as a function of number of scatterers with circle radius $a_R = 20\lambda$.

node displacement approximately equal to 25% of this average distance to the scatterers. While knowing the distance definitively in practice poses some challenges, it is possible to gain some estimate of this based on delay spreads or by using high resolution angular estimation.

Figure 5.6 plots the optimal window size as a function of the number of scatterers with the circle radius $a_R = 20\lambda$. When the number of scatterers is small (3 scatterers), the optimal window size is small. As the number of scatterers increases, so does the optimal

Table 5.1: MSE between CMD for Estimated Covariance Using Average Window Size and That Using Optimal Window Size for Each Value of a_R.

Circle Radius a_R (λ)	10	15	20	25	30	35	40	50	70	100
MSE (%)	3.73	3.4	1.31	1.92	1.36	1.5	1.16	1.28	1.59	1.91

window size. However, once the number of scatterers passes a certain value, the window size reaches an approximate upper value. This result may be explained by recognizing that as the multipath richness increases, more data is required to estimate this complexity in the spatial structure. However, once the number of scatterers gets larger than 20, the covariance begins to approach that achieved for a uniform distribution of multipaths, leading to little change with increasing richness. For $a_R = 20\lambda$, the optimal window size is approximately 13λ.

In summary, for a few scatterers, the optimal window size is approximately 25% of the average distance to the scatterers. As the number of scatterers increases, however, a larger window size is required. This window size goes up to a value of approximately 60% of the average distance to the scatterers.

5.1.4 CMD Agreement Using the Criterion of MMSE

So far we have determined the appropriate window size under different environments by considering the average rate of change of the covariance. As we discussed in Chapter 4, MSE can be used to analyze the accuracy of the derivative criterion χ, but can also be used as a criterion for finding the optimal window size since our ultimate goal is to minimize this MSE.

Thus, we explore CMD agreement using the criterion of MMSE based on the same two-ring propagation model. The simulations again use 1000 realizations of the channel model. Figure 5.7 shows the CMD as a function of displacement for $a_R = 20\lambda$ and 50λ. The results reveal that with the appropriate window size, the CMD of the estimated covariance closely matches that of the analytical covariance. Thus, the MMSE method for determining the appropriate window size is as effective as the method based on the average derivative.

Table 5.2: Comparison of Optimal Window Size between Two Methods.

Circle Radius a_R (λ)	20	40	50
Optimal Window Size by χ (λ)	5.4	9.6	12.4
Optimal Window Size by $MMSE$ (λ)	5.8	10.2	12.2

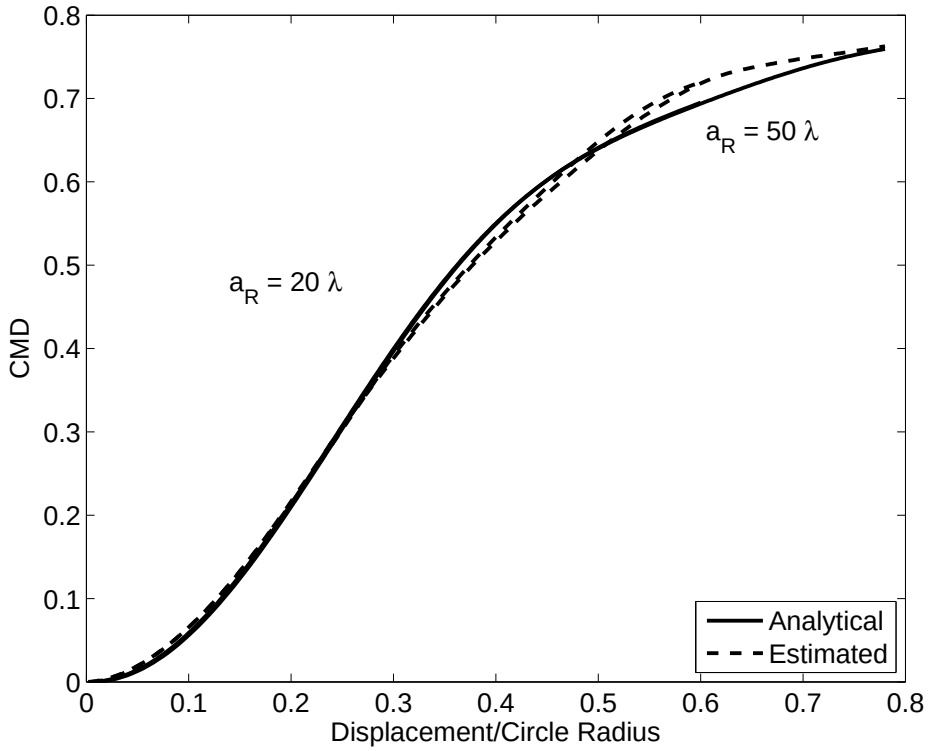

Figure 5.7: Average CMD for two different a_R as a function of displacement, with the estimated covariance obtained using the optimal window size achieved by MMSE criterion.

Furthermore, we compare the optimal window sizes obtained based on the MMSE criterion to those achieved based on matching the average CMD variation for different values of a_R in Table 5.2. The results show that the optimal window sizes obtained by those two methods are very similar for all values of a_R.

5.2 Simulations Based on Ray-Tracing Data

Given this framework for determining the optimal window size based on a simple propagation model, we now turn attention to application of the method to more realistic propagation data obtained from ray-tracing.

5.2.1 Description of Ray-Tracing Data

The simulation is performed in a three dimensional urban environment along a non-line of sight route. The transmitter is located on a street while the receiver moves along

another street which is perpendicular to the street where the transmitter is located. The sampling distance is 1/10 wavelength (1.2cm for 2.5GHz frequency) and the total distance over which the receiver moves is 1000 wavelengths (approximately 120m).

At each sample location, the number of rays received at the receiver and the coordinates (x, y, z) of the receiver are recorded. For each ray received, the complex electric field value, the delay time in seconds, the path angle of departure and the path angle of arrival are recorded.

Since the receiver is positioned close to the transmitter at the beginning of the route, there are more rays in the initial part of the record (approximately 20 rays) than there are in the later part (approximately 5 rays). The entire record consists of samples at 10059 receiver locations.

5.2.2 Processing of the Data

Since the record is so large and covers such a large displacement, we subdivide the record into shorter records each containing approximately 500 samples. Utilizing the data recorded in these sub-records, we calculate the analytical covariance using Equation (3.7) as well as from the channel realizations obtained using Equation (4.1). We next compute the CMD of the analytical covariance and that from the covariance estimated from observed channels using a sample mean over a window. We then apply the two criteria (χ and MMSE) to determine the optimal window size for covariance estimation.

Due to computational inaccuracies and abrupt changes in multipath, the observed data displays abrupt changes in the observed covariance. We therefore preprocess the data by smoothing the curves using a spline function to remove these discontinuities.

5.2.3 CMD Agreement Results and Analysis

Using our two methods, we obtain the optimal window size for each sub-record of the data and average these window sizes over the sub-records. This procedure leads to average window sizes of 16λ and 17λ (approximately 2m) for matching the slope and minimizing the MMSE, respectively. Once again, for this more realistic environment, we observe that the two methods yield very similar results. Figures 5.8 and 5.9 show the CMD agreement using

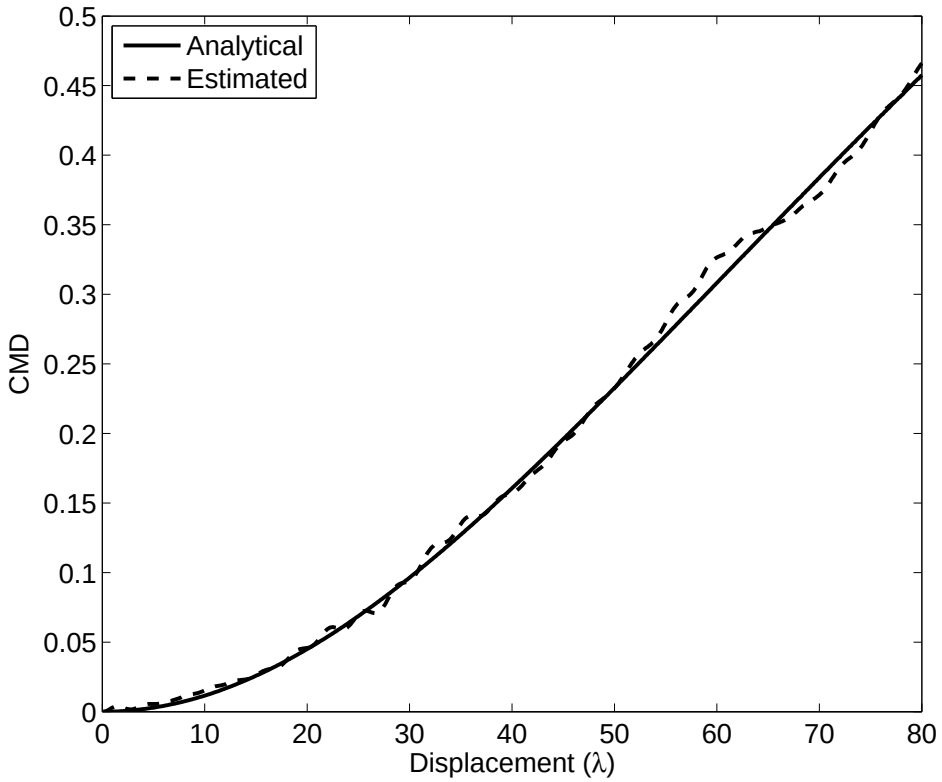

Figure 5.8: CMD as a function of receiver displacement, with the estimated covariance obtained using the optimal window size which is achieved by the criterion of average variation.

the two methods respectively for a window size of 2m. The agreement in the CMD reveals the effectiveness of our developed approach for determining the window size.

5.3 Summary of the Simulation Results

This chapter has used analysis based on a two-ring propagation model to demonstrate that the window size determined by matching the average slope of the CMD curves or minimizing the MSE of these curves are very similar. Furthermore, these window sizes lead to CMD curves that closely match those obtained using the analytical model.

The analysis explored the impact of the distance from the receiver to the scatterers as well as the number of scatterers. Even though different circle radii lead to different optimal window sizes, the ratio of the window size to the circle radius remains approximately constant, allowing us to use a single value of this normalized window size to reasonably estimate

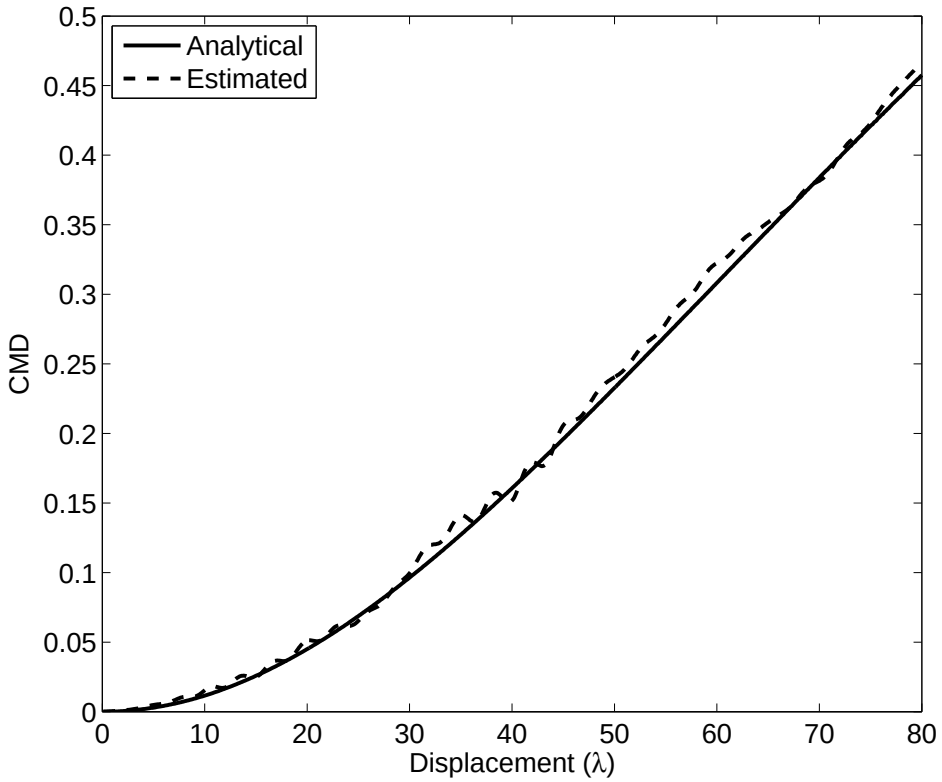

Figure 5.9: CMD as a function of receiver displacement, with the estimated covariance obtained using the optimal window size which is achieved by the criterion of MMSE.

the covariance. As the number of scatterers increases, so does the optimal window size. However, the window size reaches an upper value once the number of scatterers surpasses a certain value.

Finally, the two methods for determining the appropriate window size have been used on ray-tracing data. Again, the two methods achieve similar results. The agreement between the CMD of the estimated and analytical covariance methods demonstrates that the methods are effective for determining the appropriate window size for covariance estimation.

Chapter 6

Conclusion

This thesis derives a closed-form analytical model allowing estimation of the full MIMO channel covariance, as opposed to the more traditional one-sided or separable covariance, based on knowledge of the PAS of the channel and the antenna radiation patterns. This solution allows us to explore the dynamic nature of the channel spatial covariance matrix under time-varying channel conditions characterized by changes in the multipath spatial structure. Having such a tool is important, since it allows definition of the covariance at a point in space (or time). Otherwise, computing the covariance from a sample mean when the underlying channel statistics might be changing becomes an ill-defined problem.

The thesis also reviews the CMD [24] as a metric for measuring the relative change in the covariance as a function of node position. The work extends the usage of CMD to explore the slowly changing behavior of the channel covariance as a function of node position, and moreover to estimate a spatial window over which the sample mean should be performed for approximating the channel covariance from observed channel data.

A two-ring propagation model is introduced and used as a basis for simulation in this thesis. The propagation model is simple but provides a good foundation for studying the nature of the changing channel covariance and a starting point for practical exploration of this topic. Based on channels realized using this model, the thesis demonstrates the sensitivity of the covariance rate of change to the size of the window used to estimate the covariance, motivating the development of two approaches determining the appropriate window over which the covariance should be estimated for non-WSS time-varying channels. These two approaches compare covariance matrices computed using the analytical model and those estimated from observed channel samples utilizing different criteria: average variation of the covariance and MMSE between CMD curves as a function of node position. The

effectiveness of the methods is explored through simulation based on the two-ring propagation model. These simulations reveal that the two methods for window size estimation achieve a covariance whose CMD closely matches that achieved by the analytical solution.

More simulations are performed in this thesis, with results of both approaches matching closely. The simulations consider several different environments, which are represented by the average distances between the scatterers and the communication nodes (or the radius of the scatterer circle) and by the number of scatterers. The analysis shows that although the window size required for covariance estimation increases with the radius of the scatterer circle, the window size normalized by the circle radius remains relatively constant. This provides a possibility of estimating the covariance from the observed channels by using the average normalized optimal window size. If we have an estimate of the average distance between the scatterers and the communication node, we should compute the covariance over a node displacement approximately equal to 25% of this average distance to the scatterers.

Similarly, the window size increases with the number of scatterers (multipath richness). However, once the richness surpasses a certain level, the window size approximately achieves a maximum value.

Finally, the thesis shows simulations based on ray-tracing data. After a description of the ray-tracing data, the thesis discusses sub-division of the data into multiple records and data smoothing. Application of the methods outlined in this thesis show that the CMD from the estimated covariance matches that from the analytical covariance for a window size of approximately 16 wavelengths.

The framework in this thesis provides a capability that allows us to better understand practical computation of channel spatial covariance matrices for channel modeling and MIMO signal processing applications. However, significant future research work could be completed. Through the understanding of the dynamic behavior of the covariance, channel matrices could then be realized and a usable channel model therefore could be defined. This thesis suggests computing the covariance over a spatial window size of approximately one fourth of the average distance to the scatterers. But knowing this distance definitively poses some challenges in practice. In future research it is possible to gain some estimate of this based on delay of spreads or by using high resolution angular estimation. Similarly,

the determination of the number of scatterers around the communication node is also challenging in real communication system design. However, it is still possible to estimate this through related techniques. MIMO signaling scheme design could also take advantage of the results shown in this thesis to reduce the frequency of CDI feedback without significant loss of throughput.

Bibliography

[1] G. J. Foschini, "Layered space-time architecture for wireless communication in a fading environment when using multi-element antennas," *Bell Labs Tech. J.*, vol. 1, no. 2, pp. 41–59, 1996. 1

[2] L. Zheng and D. N. C. Tse, "Diversity and multiplexing: A fundamental tradeoff in multiple-antenna channels," *IEEE Transactions on Information Theory*, vol. 49, no. 5, pp. 1073–1096, 2003. 1, 5

[3] J. H. Winters, "On the capacity of radio communication system with diversity in a Rayleigh fading environment," *IEEE J. Select Areas Communication*, vol. SAC-5, pp. 871–878, 1987. 1

[4] G. J. Foschini and M. J. Gans, "On limits of wireless communications in a fading environment when using multiple antennas," *Wireless Personal Communications*, vol. 6, pp. 311–335, 1998. 1

[5] A. Goldsmith, S. A. Jafar, N. Jindal, and S. Vishwanath, "Capacity limits of MIMO channels," *IEEE Journal on Selected Area in Communications*, vol. 21, no. 5, pp. 684–702, 2003. 1, 5

[6] A. L. Anderson, J. R. Zeidler, and M. A. Jensen, "Stable transmission in the time-varying MIMO broadcast channel," *EURASIP Journal on Advances in Signal Processing, Special Issue on MIMO Transmission with Limited Feedback*, vol. 2008, no. Article ID 617020, 2008. 1

[7] S. A. Jafar, S. Vishwanath, and A. Goldsmith, "Channel capacity and beamforming for multiple transmit and receive antennas with covariance feedback," *Communications,2001.ICC2001.IEEE International Conference on*, vol. 7, pp. 2266–2270, 2001. 1, 6, 7, 8

[8] H. Xu, D. Chizhik, H. Huang, and R. Valenzuela, "A generalized space-time multiple-input multiple-output (MIMO) channel model," *IEEE Transactions on Wireless Communications*, vol. 3, no. 3, pp. 966–975, 2004. 2

[9] Q. Li, J. Zhu, Q. Li, and C. N. Georghiades, "Efficient spatial covariance estimation for asynchronous co-channel interference suppression in MIMO-OFDM systems," *IEEE Transactions on Wireless Communications*, vol. 7, no. 12, pp. 4849–4853, 2008. 2

[10] J. Wallace, H. Ozcelik, M. Herdin, E. Bonek, and M. Jensen, "Power and complex envelope correlation for modeling measured indoor MIMO channels: A beamforming

evaluation," *The IEEE 58th Vehicular Technology Conference 2003, VTC 2003-Fall*, vol. 1, pp. 363–367, 2003. 2

[11] A. L. Anderson, J. R. Zeidler, and M. A. Jensen, "Reduced-feedback linear precoding with stable performance for the time-varying MIMO broadcast channel," *IEEE Journal on Selected Areas in Communications*, vol. 26, no. 8, pp. 1483–1493, 2008. 2, 8, 9, 10, 13

[12] E. Visotsky and U. Madhow, "Space-time transmit precoding with imperfect feedback," *IEEE Transactions on Information Theory*, vol. 47, no. 6, pp. 2632–2639, 2001. 2, 8, 9, 13

[13] M. A. Jensen, Y. Shi, and Y. Yang, "Channel covariance modeling for multi-user MIMO systems," *Antennas and Propagation (EuCAP), 2010 Proceedings of the Fourth European Conference on*, pp. 1–5, Aprial 2010. 2

[14] Y. Shi and M. A. Jensen, "Stable transmission in the frequency-selective MIMO broadcast channel," *Vehicular Technology Conference, 2008. VTC 2008-Fall. IEEE 68th*, pp. 1–5, 2008. 6

[15] S. A. Jafar and A. Goldsmith, "Multiple-antenna capacity in correlated Rayleigh fading with channel covariance information," *IEEE Transactions on Wireless Communications*, vol. 4, no. 3, pp. 990–997, 2005. 7

[16] A. Soysal and S. Ulukus, "Optimum power allocation for single-user MIMO and multi-user MIMO-MAC with partial CSI," *IEEE Journal on Selected Areas in Communications*, vol. 25, no. 7, pp. 1402–1412, 2007. 8

[17] C. Oestges, "Validity of the Kronecker model for MIMO correlated channels," *Vehicular Technology Conference, 2006. VTC 2006-Spring. IEEE 63th*, pp. 2818–2822, 2006. 10, 12

[18] L. Wood and W. S. Hodgkiss, "On the performance of analytical channel models in capturing channel correlation structure," *Vehicular Technology Conference, 2008. VTC 2008-Fall. IEEE 68th*, pp. 1–5, 2008. 10, 13

[19] D.-S. Shiu, G. J. Foschini, M. J. Gans, and J. M. Kahn, "Fading correlation and its effect on the capacity of mutielement antenna systems," *IEEE Transactions on Communications*, vol. 48, no. 3, pp. 502–513, 2000. 11

[20] H. Özcelik, M. Herdin, W. Weichselberger, J. Wallace, and E. Bonek, "Deficiencies of 'Kronecker' MIMO radio channel model," *Electronics Letters*, vol. 39, no. 16, pp. 1209–1210, 2003. 11, 12

[21] W. Weichselberger, M. Herdin, H. Özcelik, and E. Bonek, "A stochastic MIMO channel model with joint correlation of both link ends," *IEEE Transactions on Wireless Communications*, vol. 5, no. 1, pp. 90–100, 2006. 12

[22] J. W. Wallace and M. A. Jensen, "Time-varying MIMO channels: Measurement, analysis, and modeling," *IEEE Transactions on Antennas and Propagation*, vol. 54, no. 11, pp. 3265–3273, 2006. 17

[23] M. Herdin and E. Bonek, "A MIMO correlation matrix based metric for characterizing non-stationarity," *Proceedings IST Mobile and Wireless Communications Summit*, 2004. 19

[24] M. Herdin, N. Czink, H. Özcelik, and E. Bonek, "Correlation matrix distance, a meaningful measure evaluation of non-stationary MIMO channels," *Vehicular Technology Conference,2005.VTC 2005-Spring.2005 IEEE 61st*, vol. 1, pp. 136–140, 2005. 20, 21, 45

[25] N. Czink, B. Bandemer, G. Vazquez-Vilar, L. Jalloul, C. Oestges, and A. Paulraj, "Spatial separation of multi-user MIMO channels," *Personal, Indoor and Mobile Radio Communications, 2009 IEEE 20th International Symposium on*, pp. 1059–1063, 2009. 20